UNCLASSIFIED

AD NUMBER

AD911383

NEW LIMITATION CHANGE

TO

Approved for public release, distribution unlimited

FROM

Distribution authorized to U.S. Gov't. agencies only; Test and Evaluation; APR 1973. Other requests shall be referred to Air Force Avionics Laboratory, Attn: NVT-1, Wright-Patterson AFB, OH 45433.

AUTHORITY

AFWAL ltr, 28 Nov 1984

THIS PAGE IS UNCLASSIFIED

AD **911383**

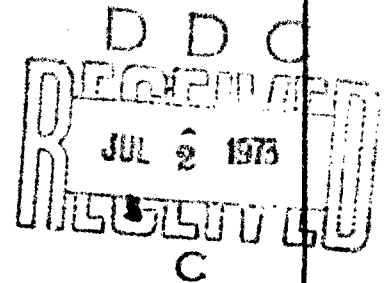AUTHORITY: *AFWAL ltr, 28 Nov 84*

AFAL-TR-73-179

COMPARISON OF APPROXIMATE METHODS
FOR AIRBORNE GUNNERY BALLISTICS CALCULATIONS

John M. Norwood

Applied Research Laboratories
The University of Texas at Austin

TECHNICAL REPORT AFAL-TR-73-179

April 1973

DDC

JUL 2 1975

C

Best Available Copy

NOTICE

COMPARISON OF APPROXIMATE METHODS
FOR AIRBORNE GUNNERY BALLISTICS CALCULATIONS

John M. Norwood

FOREWORD

This technical report is submitted in accordance with the requirements of Contract F33615-70-C-1162, Exhibit B, Sequence No. B002. The work documented herein was accomplished under Project 7629, Task 03 during the period April 1971 to October 1971, under the cognizance of Mr. Leo Krautmann, Project Engineer, AFAL/NVT-1, Air Force Avionics Laboratory, Wright-Patterson Air Force Base, Ohio.

The studies upon which this report is based were done by the Aerospace Technology Division, Applied Research Laboratories, The University of Texas at Austin, Austin, Texas, and were published previously as three UT/ARL Technical Memorandums.

This report was submitted by the author for approval in April 1973, and is assigned originator's report number UT/ARL-TR-73-10.

This report has been reviewed and is approved for publication.

WILLIAM J. DELANEY, Colonel, USAF
Chief, Navigation and
Weapon Delivery Division

ABSTRACT

Practical bounds on computer capacity and computation time dictate a need for simplified methods of airborne gunnery ballistics computation particularly under conditions which involve large ballistic yaw. The projectile trajectory data needed for on-board solution of the fire control problem can be obtained in two ways: (1) trajectory computation on board the aircraft, (2) curve fitting precomputed trajectory data. This report contains a comparison of two approaches to on-board trajectory computation and polynomial curve fitting of precomputed trajectory data.

A new, simplified set of approximate, large-yaw, ballistic trajectory equations are derived for airborne gunnery applications in which corrections for yaw drag and windage jump are included. The results of computations done with the new set of equations are in excellent agreement with the results of calculations done with the approximate equations used at Eglin Air Force Base to generate trajectory tables. Comparisons are made for the 20-mm, M56 round. A reduction in computer time by a factor of 15 to 20 (depending on firing geometry) over the Eglin set of equations can be expected when the simplified set of equations is used. The new set of equations is almost as simple as particle trajectory equations and is a candidate set for on-board calculations.

When the yaw-drag and windage-jump corrections are used with the Siacci method, a closed-form solution to the ballistic trajectory equations is obtained. This method is almost as accurate as the simplified set of equations above, except for time-of-flight calculations. It is sufficiently accurate for air-to-air applications out to a range of approximately 3000 ft. If time of flight is not important, as, for example, in air-to-ground applications, then this method yields results of sufficient accuracy out to moderate ranges for most geometries. Also, this method appears to be 20 to 100 times as fast as point-mass integration and 500 to 1500 times as fast as numerical integration of the Eglin approximate equations of motion.

A method of polynomial curve fitting of ballistic lead angles for air-to-ground applications is presented. This method may be useful in situations where on-board calculations are not possible.

TABLE OF CONTENTS

LIST OF ILLUSTRATIONS

LIST OF TABLES

LIST OF SYMBOLS

a — Windage jump constant $(X = 10^3 a \delta_o)$

a_i — Coefficients for curve fit of S vs U

a_o — The ratio of the speed of sound at firing altitude to that at sea level

A — Depending upon context, axial moment of inertia of the projectile or the turret traverse angle

$A(U)$ — Siacci altitude function

$A_{ijk\ell}$ — Polynomial curve-fit coefficient

A_G — Gun deflection angle (Fig. 7)

A_T — Line-of-sight deflection angle to the target

A_Z — Gun azimuth angle (Fig. 8)

b — Depending upon context, windage jump constant $(X = 10^3 b \delta_o)$, or dependent variable in the general symbolic equation for the polynomial curve fit

b_i — Coefficients of the curve fits of Siacci functions $T(S)$, $I(S)$, and $A(S)$

B — Depending upon context, transverse moment of inertia of the projectile, or the azimuth angle of $\bar{u}_o$ measured between the x and ξ axes

c — $= c' + \dfrac{c''}{s_o - 1}$

c' — $= \dfrac{\rho_o d^2}{2m} \left[K_L + \dfrac{md^2}{B} K_H \right]$

c'' — $= \dfrac{\rho_o d^2}{2m} K_{D_o}$

C — $= \dfrac{m}{144 d^2}$, the ballistics coefficient (lb/in.^{2}) or the inverse of the matrix W, depending upon context

ix

$\vec{C}$	Constants over a trajectory ($\vec{S} = \vec{C} P$)
C_ξ, C_η, C_ζ	Components of $\vec{C}$ in the ξ, η, ζ coordinate system
d	Projectile diameter
D	$= dQ/dP$, or the inverse of the matrix X, depending upon context
E	$= \rho d^2 V K_D$, or the turret depression angle, of the inverse of the matrix Y, depending upon context
E_G	Gun depression angle (Fig. 7)
E_L	Gun depression angle (Fig. 8)
E_o	$= \rho d^2 V K_{D_o}$
E_T	Line-of-sight depression angle to the target
F	Inverse of the matrix Z
g	$= 32.174$ ft/sec^2, acceleration due to gravity
$\vec{G}$	Aerodynamic torque on the projectile
$G(U)$	$= \dfrac{U K_{D_o} (U/B_o)}{1883}$
h	Constant in the equation for an exponential atmosphere
$\vec{H}$	Angular momentum of the projectile
I	Number of data points required for w in polynomial curve fit
$I(U)$	Siacci inclination function
J	Number of data points required for x in polynomial curve fit
k	Constant ($\delta = K\delta_o e^{-kP}$)

k_o	$= K_{D_\delta 2} K$
K	Constant $(\delta = K \delta_o e^{-kP})$, or number of data points required for y in polynomial curve fit, depending upon context
K_D	Drag force coefficient
K_{D_o}	Zero-yaw drag force coefficient
$K_{D_\delta 2}$	Yaw-drag force coefficient
K_F	Magnus force coefficient
K_H	Damping moment coefficient
K_L	Lift force coefficient
K_M	Overturning moment coefficient
K_T	Magnus moment coefficient
L	Number of points required for z in polynomial curve fit
m	Projectile mass
M	Mach number
N	Angular velocity of projectile about the spin axis
N_a	Normalization constant for polynomial curve fit
P	Pseudorange
Q	Gravity drop
s_o	$= \dfrac{A^2 N^2}{4B \rho d^3 V K_M}$, static stability factor
S	Swerve

S_ξ, S_η, S_ζ — Components of $\vec{S}$ in the ξ, η, ζ coordinate system

S_x, S_y — Components of $\vec{S}$ in and perpendicular to the plane of yaw, respectively

$S(U)$ — Siacci space function

t — Time

$T(U)$ — Siacci time function

u — $= \dot{P}$, the projectile pseudovelocity

$\vec{u}_o$ — $= \vec{V}_o$, initial projectile velocity

U — $= u/a_o$

$\vec{V}$ — Projectile velocity

$\vec{V}_A$ — Aircraft velocity (TAS)

$\vec{V}_m$ — Muzzle velocity

$\vec{V}_o$ — Projectile initial velocity

V_{ox}, V_{oy}, V_{oz} — Components of $\vec{V}_o$ in the x, y, z system

V_{sd} — $= 1116.45$ ft/sec, the speed of sound at sea level for a standard atmosphere

V_{xy} — $= \sqrt{V_{ox}^2 + V_{oy}^2}$

w — Independent variable in the polynomial curve fit

W — Matrix (w_p^i)

x — Independent variable in the polynomial curve fit

X — Component of windage jump in the plane of yaw, or the matrix (x_q^j), depending upon context

xii

LIST OF SYMBOLS (concluded)

y	Independent variable in the polynomial curve fit
y_A	Aircraft altitude
y_T	Target altitude
Y	Component of windage jump perpendicular to the plane of yaw, or the matrix (y_r^k), depending upon context
z	Independent variable in the polynomial curve fit
Z	Matrix (z_s^ℓ)
δ	Yaw angle (angle of attack)
δ_o	Initial yaw
θ_o	Angle of elevation of $\vec{P}$ or $\vec{V}_o$ above the horizontal
ν	$= Nd/V$, dimensionless spin
ξ, η, ζ	Air-mass coordinate system
ρ	Air density
ρ_o	$= 0.07674 \text{ lb/ft}^3$, air density at sea level
σ	$= \rho/\rho_o$, relative air density
ϕ	Projectile precession angle
ϕ'	$= \phi - \phi_o$
ϕ_o	Initial precession angle
ΔA	Deflection ballistic lead angle
ΔE	Depression ballistic lead angle
$\Delta \xi$	Difference in ξ between approximate theory of this report and that of Ref. 1
$\Delta \zeta$	Difference in ζ between approximate theory of this report and that of Ref. 1

SECTION I

INTRODUCTION

1. Onboard Trajectory Computations for Large-Yaw Situations

The use of side-firing or flexible gunnery systems in modern airborne applications introduces the problem of large-yaw ballistics. Fixed, side-firing guns are used in the gunship application and the use of flexible (turreted) systems is anticipated. The problem also occurs to a lesser extent in modern fixed-gun fighter applications in high angle-of-attack situations.

The problem of large-yaw ballistics arises in airborne applications whenever the gun-pointing direction lies significantly away from the direction of motion of the aircraft. When this occurs, the spin axis of the projectile, which coincides with the gunbore line, does not coincide with the direction of motion of the projectile. The angle between the projectile velocity vector and spin axis is known as the projectile angle of attack or the yaw angle. The effect of nonzero yaw upon the projectile is to produce aerodynamic moments at right angles to the spin axis. The behavior of the spinning projectile under the influence of these moments is much like that of a gyroscope, or a top, under the influence of gravity. The projectile precesses about its velocity vector.

Nonzero yaw also induces aerodynamic forces at right angles to the velocity vector, namely the lift and Magnus forces. The lift force is in the plane containing the projectile spin axis and velocity vector (the plane of yaw) and its effect is analogous to the effect of the lift force on an airplane. For the case of a spinning projectile, however, the lift force precesses with the projectile about the velocity vector. This is analogous to an airplane in a barrel roll. The Magnus force is perpendicular to the plane of yaw and behaves in a similar fashion. Under the influence of these forces (mainly the lift, which is considerably larger than the Magnus force), the projectile executes a sort of spiraling motion as it moves downrange. For a dynamically stable projectile, the yaw angle rapidly dies out and the spiraling motion stops. The total effect is to deflect the trajectory away from its original direction by a small amount. This effect is the swerve, or the windage jump, and, as a rule of thumb, it amounts to about a milliradian (mr) of deflection per degree of projectile initial yaw. For example, for an F-4 in a dogfight, flying at 800 ft/sec, and with an angle of attack of the gun of 15 deg, the initial yaw angle of the projectile is about 3 deg and the trajectory will be deflected about 3 mr to the right.

The aerodynamic drag is also increased by nonzero yaw. This increase, referred to as the yaw drag, tends to slow the projectile down at a faster rate and increases the time of flight. This increase in time

1

of flight is not considered significant in air-to-ground situations, but may be important in air-to-air encounters. In air-to-ground situations, the shape of the trajectory is not altered to a significant extent and it does not hurt if the projectile arrives "a little late." In air-to-air situations, the target is moving at a high rate and small errors in the time of flight may result in erroneous kinematic predictions and large miss distances.

The motion of a spinning projectile with large yaw can, of course, be determined by means of numerical integration of the six-degree-of-freedom equations provided appropriate aerodynamic data is available. However, the computation of trajectory tables may require excessive computer time even at ground-based computer facilities. Onboard solution of the six-degree-of-freedom equations in real-time fire-control applications is not considered possible using current technology. It may be possible with large-scale integrated circuits (LSI), but this problem has not been investigated to the author's knowledge.

The trajectory table problem for the 20-mm, M56 round was solved by use of the set of approximate equations which are documented in Ref. 1 and which do not require much computer time. These approximate equations have been written in FORTRAN as code R370 for the computer at Eglin Air Force Base by Eglin personnel. The equations are still unsuitable for onboard use, however.

This report contains two approaches to the problem of onboard trajectory computation which are reasonably accurate for the 20-mm, M56 round and which do not require excessive computer time. These methods involve approximate methods for treating windage jump and handling yaw drag.

In the first method to be described, a yaw drag correction is added to the point-mass equations, and windage jump is accounted for by utilization of the results of calculations done with the equations of Ref. 1. The second method is the Siacci method with a yaw drag correction and with the same windage jump correction used in the first method.

The method of treating windage jump was suggested for use with the Siacci method in Ref. 2, and an investigation of its utilization is reported herein and in Ref. 3. A natural extension is to use the same windage jump equations with point-mass calculations; this was done and the results are reported herein and in Ref. 4.

The yaw-drag correction is that of Sterne (Refs. 5 and 6). It was originally applied to the Siacci method and its use has been extended to the modified point-mass calculations herein and in Ref. 4.

The equations of the first method which are derived herein and in Ref. 4 are

2

$$m \frac{du}{dP} = -\rho d^2 V K_{D_o} \left(V/V_{sd}\right)\left[1 + k_o e^{-kP}\right]$$

$$\frac{dt}{dP} = \frac{1}{u}$$

$$\frac{dD}{dP} = \frac{g}{u^2}$$

$$\frac{dQ}{dP} = D$$

where

$$V = u \sqrt{1 - 2D \sin \theta_o + D^2}$$

P is the pseudorange, Q is the gravity drop, t is the time, $u = dP/dt$ is the pseudovelocity, m is the projectile mass, d is the projectile diameter, ρ is the air density, V is the projectile velocity, V_{sd} is the velocity of sound, g is the acceleration due to gravity, K_{D_o} is the zero-yaw drag, k_o and k are constants, and θ_o is the angle of elevation of $\vec{P}$ above the horizontal. These equations are related to a rectangular air-mass coordinate system ξ, η, ζ by the relations

$$\xi = P \cos \theta_o + C_\xi P$$

$$\eta = P \sin \theta_o - Q + C_\eta P$$

$$\zeta = C_\zeta P$$

where $C_\xi P$, $C_\eta P$, and $C_\zeta P$ are components of swerve (windage jump); C_ξ, C_η, and C_ζ are calculated from initial conditions and are constants for any given trajectory.

To an individual familiar with the six-degree-of-freedom equations, the simplicity of this set of relations is obvious. The advantage of using P as the independent variable rather than t lies in the fact that fewer

integration steps are required to integrate out to a given range, so computer time is reduced. One might add that these equations would be particle trajectory (point-mass) equations if the term

$$\left[1 + k_o e^{-kP}\right]$$

were deleted. They are applicable with greater accuracy wherever particle equations are useful. The possibility of onboard numerical integration of particle trajectories has been demonstrated in the F-111D Mk II avionics and in the Hot Line applications.

In the second method (the modified Siacci method) the equations of motion as described above are replaced by the following set:

$$S(u/a_o) = S(u_o/a_o) + \frac{\sigma}{C}P + \frac{k_o}{2cC}$$

$$Q = \left(\frac{C}{\sigma a_o}\right)^2 \left[A(u/a_o) - A(u_o/a_o) - I(u_o/a_o)\frac{\sigma}{c}P\right]$$

$$t = \frac{C}{\sigma a_o}\left[T(u/a_o) - T(u_o/a_o)\right]$$

where C is the ballistic coefficient, a_o is the ratio of the speed of sound at altitude to that at sea level, σ is the relative air density ($\sigma = \rho/\rho_o$ where ρ_o is the air density at sea level), and c is a constant. S, T, I, and A are functions tabulated against U. The term $k_o/2cC$ is the yaw drag correction first derived, presumably, by Sterne. The windage jump correction employed with the Siacci equations is the same as that described above. Siacci ballistic computations are valid for large-yaw, moderate-range trajectories of the 20-mm, M56 round. Applicable for both air-to-air and air-to-ground fire control, the Siacci method yields a substantial reduction in computation time over numerical integration of the equations of motion. The basic argument for implementation of the Siacci ballistics equations for onboard fire control computation is that updating of ballistic lead angles may be performed in a shorter time interval than can be accomplished by numerical integration, thus, reducing the error imposed by failure to obtain instantaneous lead information in a time-dependent environment. In the air-to-air case, reduction in ballistic computation time affords more time for processing of kinematic lead data and other necessary functions of the fire control computer.

4

Siacci theory is an approximation to the point-mass equations of motion of a projectile. The basic assumption is that the velocity of the projectile in the direction of the initial velocity vector is equal to the actual projectile velocity at all points along the trajectory. The error arising from this assumption is small for short-range, relatively flat trajectories; however, the error increases with range and trajectory curvature, which limits the effective range of Siacci ballistics. For the 20-mm round, fairly good computational accuracy is maintained for ranges approaching the effective limits of the gun.

2. Lead Computation Modeling

For onboard solution of fire control problems, there are two ways to obtain projectile trajectory data. Trajectories may be numerically integrated on board the aircraft as needed or else trajectories or ballistic leads may be calculated beforehand at ground computer installations and provided as an input into the fire-control computer in the form of tables or curve fits. The method used depends upon the type of fire-control system, fire-control accuracy requirements, and physical system limitations such as computer storage size and cycle time.

If approximate trajectory calculations of one type or another as described herein are considered to be sufficiently accurate, onboard calculations are possible as demonstrated in the fire-control system in the F-111D (Mark II avaioncs) and the currently experimental Hot Line system. However, required computation time is short. In a system such as that of the F-111D, digital computation of an entire trajectory is ideally instantaneous. A practical bound on computation time, however, may be the reaction time of the pilot or about one-tenth of a second. In the Hot Line system, calculations are carried out in real time; the available calculation time is equated to the time of flight. Multiple trajectories must be integrated at once, however. For a 3-sec time of flight and a display showing 10 "tracer bullets," the available calculation time is 0.3 sec per trajectory, if trajectories are computed serially on a time-sharing basis.

When onboard calculations are not feasible, methods of curve fitting precomputed trajectory data are appropriate. This investigation is intended to aid in the design of fire-control systems for flexible air-to-ground gunnery. Such systems must have high accuracy to be effective, particularly at relatively high operational altitudes. Also, rapid computation of lead angles is essential to this high accuracy. The computational methods should also be applicable to air-to-air situations.

The use of curve-fitted trajectory data is a tradeoff. Computer time should be minimized, but more core storage capacity may be necessary. The purpose of this investigation is to determine some idea as to the amount of storage necessary and, in the process, to discover the best method of handling the trajectory data. The best method should use the least computer core space while also using minimal computer time.

5

There are a number of schemes for handling ballistics data in the airborne computer and a number of methods for curve fitting it. The most direct method would be to curve fit the trajectories themselves, but the quantities actually required in the fire-control problem are the ballistic leads in one form or another. One such method is contained herein (Section III) and in Ref. 7.

SECTION II

TRAJECTORY COMPUTATION

1. The Large-Yaw Problem

The yaw angle (angle of attack) of a projectile is the angle between its longitudinal axis and its direction of motion through the air. When a projectile leaves the muzzle of a gun, its longitudinal axis orientation is that of the gun barrel or of the muzzle velocity vector $\vec{V}_m$, whereas the projectile velocity $\vec{V}_o$ is the vector sum of the muzzle velocity $\vec{V}_m$ and the aircraft velocity $\vec{V}_A$; i.e.,

$$\vec{V}_o = \vec{V}_m + \vec{V}_A$$

As can be seen from Fig. 1, the angle between $\vec{V}_o$ and $\vec{V}_m$, which is the yaw angle δ_o, can be large when the angle between $\vec{V}_A$ and $\vec{V}_m$ is large.

When the yaw angle is small, as it usually is in the fixed gun application of fighter aircraft where $\vec{V}_m$ and $\vec{V}_A$ are nearly parallel, the motion of the projectile is adequately represented by the simple equation

$$m \frac{d\vec{V}}{dt} = - E_o \vec{V} + m \vec{g} \tag{1}$$

where $\vec{V}$ is the projectile velocity, $E_o \vec{V}$ is the drag, m is the projectile mass, and $\vec{g}$ is the acceleration due to gravity. Also

$$E_o = \rho d^2 V K_{D_o}(M) \tag{2}$$

where ρ is the air density, d is the projectile velocity, K_{D_o} is the zero-yaw drag function, and M is the Mach number.

$$M = V/V_{sd} \tag{3}$$

where V_{sd} is the speed of sound.

Equation (1) accurately describes the motion of a projectile moving through the air when the yaw is zero. Additional forces such as the
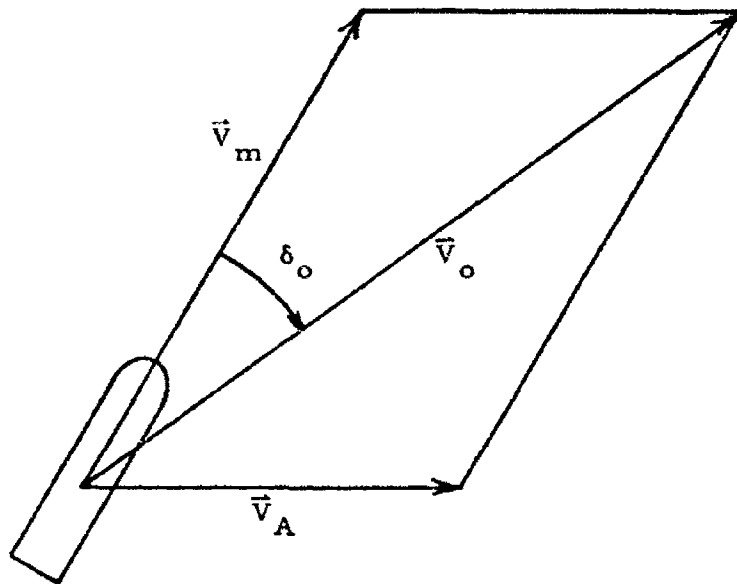
$\vec{V}_A$ = Aircraft velocity (true air speed)

$\vec{V}_m$ = Projectile muzzle velocity

$\vec{V}_o$ = Projectile velocity in the air mass

δ_o = Yaw angle (angle of attack)

Figure 1

The Initial Yaw Angle of the Projectile

8

yaw drag, the lift force, and the Magnus force result from nonzero yaw, so when the yaw is too large, Eq. (1) is no longer a good approximation.

The lift and Magnus forces are at right angles to the projectile velocity vector and contribute to the swerve (or the windage jump). The swerve is the deviation of the true trajectory from the one described by Eq. (1). The yaw-drag force is in the opposite direction to $\vec{V}$ and tends to increase the projectile time of flight between gun and target.

The time history of the yawing motion of a projectile is given by the equation

$$\frac{d\vec{H}}{dt} = \vec{G} \tag{4}$$

where $\vec{H}$ is the angular momentum vector of the projectile and $\vec{G}$ is the aerodynamic torque. $\vec{G}$ includes the Magnus moment, the overturning moment, the damping moment, and the spin deceleration moment. It is this equation which presents the major difficulty in the numerical integration of the six-degree-of-freedom equations because of the gyroscopic, nutational, and precessional motion of the projectile. Accurate description of the nutational motion requires a very small integration step size.

In order to solve the large-yaw problem, either the full set of six-degree-of-freedom equations must be utilized, or a suitable approximation must be found. Such an approximation is described in Ref. 1, where the nutational motion was eliminated from the equations. A further simplification is documented here.

2. The Approximate Equations Used in the Eglin Code

A yawed, spinning projectile does not maintain a vertical plane trajectory as is described by the point-mass equations of motion and the basic Siacci equations. Due to the angular motion of the projectile, the aerodynamic forces cause it to swerve, with components in and perpendicular to the initial plane of yaw. Examination of calculated values of the angular windage-jump components from the set of approximate equations used by Eglin Air Force Base for trajectory tabulation for the 20-mm, M56 round (Ref. 1) revealed that both angular components become essentially constant after the yaw is sufficiently damped. Further, both components are conveniently approximated as being proportional to δ_o with almost no dependence upon other initial conditions. This provided a very simple means of obtaining an accurate representation of fairly complex projectile motion. The results of Ref. 1 are summarized by the following equations (see the List of Symbols).

9

$$m\ddot{P} = -E\dot{P} \tag{5}$$

$$m\ddot{Q} = -E\dot{Q} + mg \tag{6}$$

$$m\ddot{S}_x = -E\dot{S}_x + \rho d^2 V^2 \left[K_L \cos \phi' + \nu K_F \sin \phi' \right] \sin \delta \tag{7}$$

$$m\ddot{S}_y = -E\dot{S}_y + \rho d^2 V^2 \left[K_L \sin \phi' - \nu K_F \cos \phi' \right] \sin \delta \tag{8}$$

$$\frac{d \cos \delta}{dt} = \frac{\rho d^2 V}{m} \left[K_L - \frac{md^2}{A} \left\{ K_T + \frac{\rho d^5}{A\nu^2} K_H K_M \right\} \right] \sin^2 \delta \tag{9}$$

$$\dot{\phi} = \frac{\rho d^3 V^2}{AN} \left[K_M - \frac{\rho d^5}{A} K_H K_T \right] \tag{10}$$

where a dot represents differentiation with respect to time,

$$E = \rho d^2 V K_D (M, \delta) \tag{11}$$

$$V = \sqrt{\dot{P}^2 - 2 \dot{P} \dot{Q} \sin \theta_o + \dot{Q}^2} \tag{12}$$

and

$$\phi' = \phi - \phi_o \tag{13}$$

Terms containing K_H can be deleted from Eqs. (9) and (10) since they are negligible.

Projectile coordinates are shown in Figs. 2 and 3. In Fig. 2, the 1, 2, 3 coordinate system is right-handed with the 1 axis along the velocity vector $\vec{V}$. The 1, 2 plane is a vertical plane containing $\vec{V}$ ($\vec{V}$ is not necessarily horizontal). The precession angle ϕ is a rotation about the 1-axis of 2 into 2' which is in the plane of yaw. The plane of yaw is the plane containing the shell axis and the velocity vector $\vec{V}$. The plane of yaw rotates about $\vec{V}$ with precession rate $\dot{\phi}$.
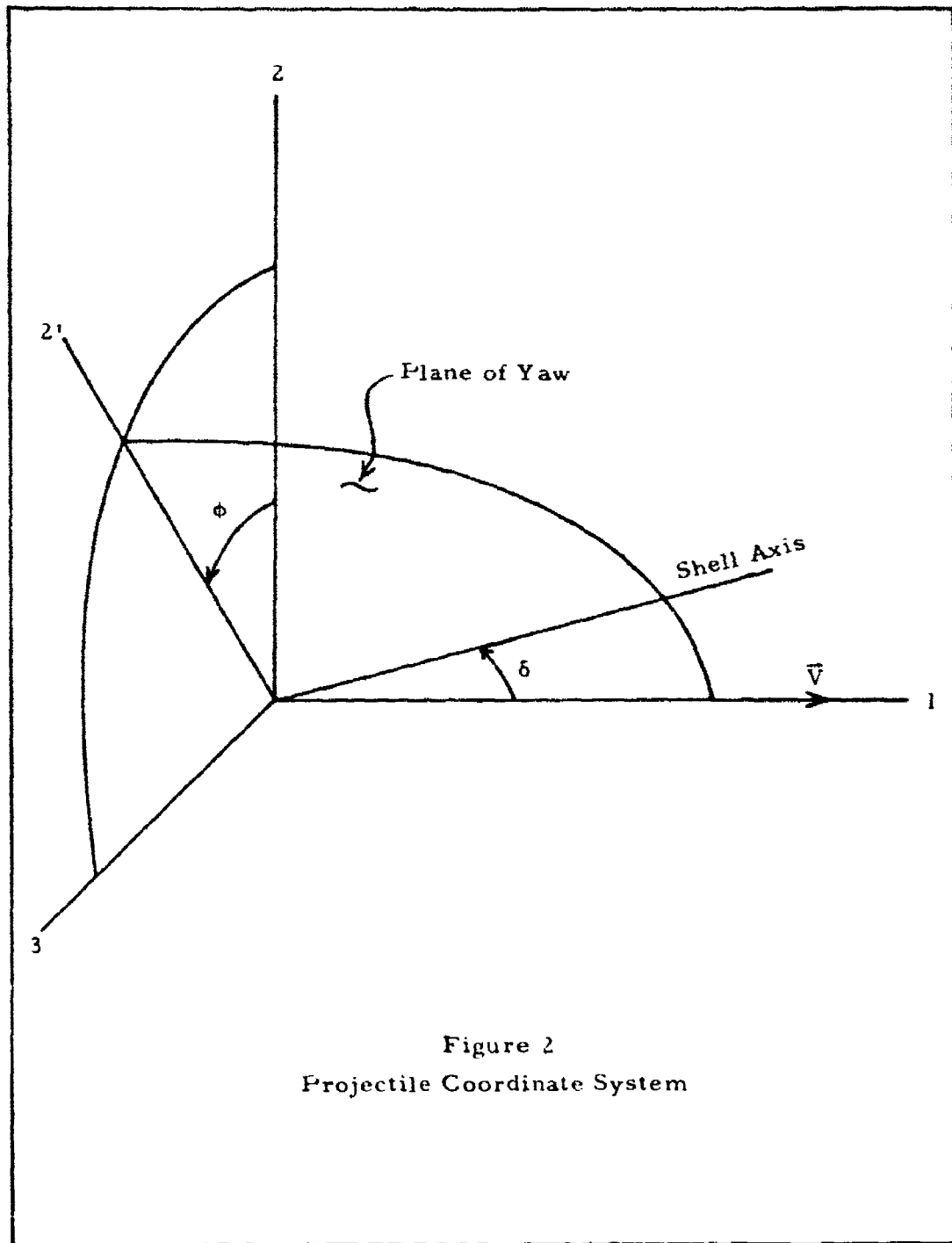
Figure 2
Projectile Coordinate System

Figure 3

Siacci Projectile Coordinates

($\vec{P}$ is in the ξ, η plane and $\vec{S}$ is perpendicular to $\vec{P}$.)
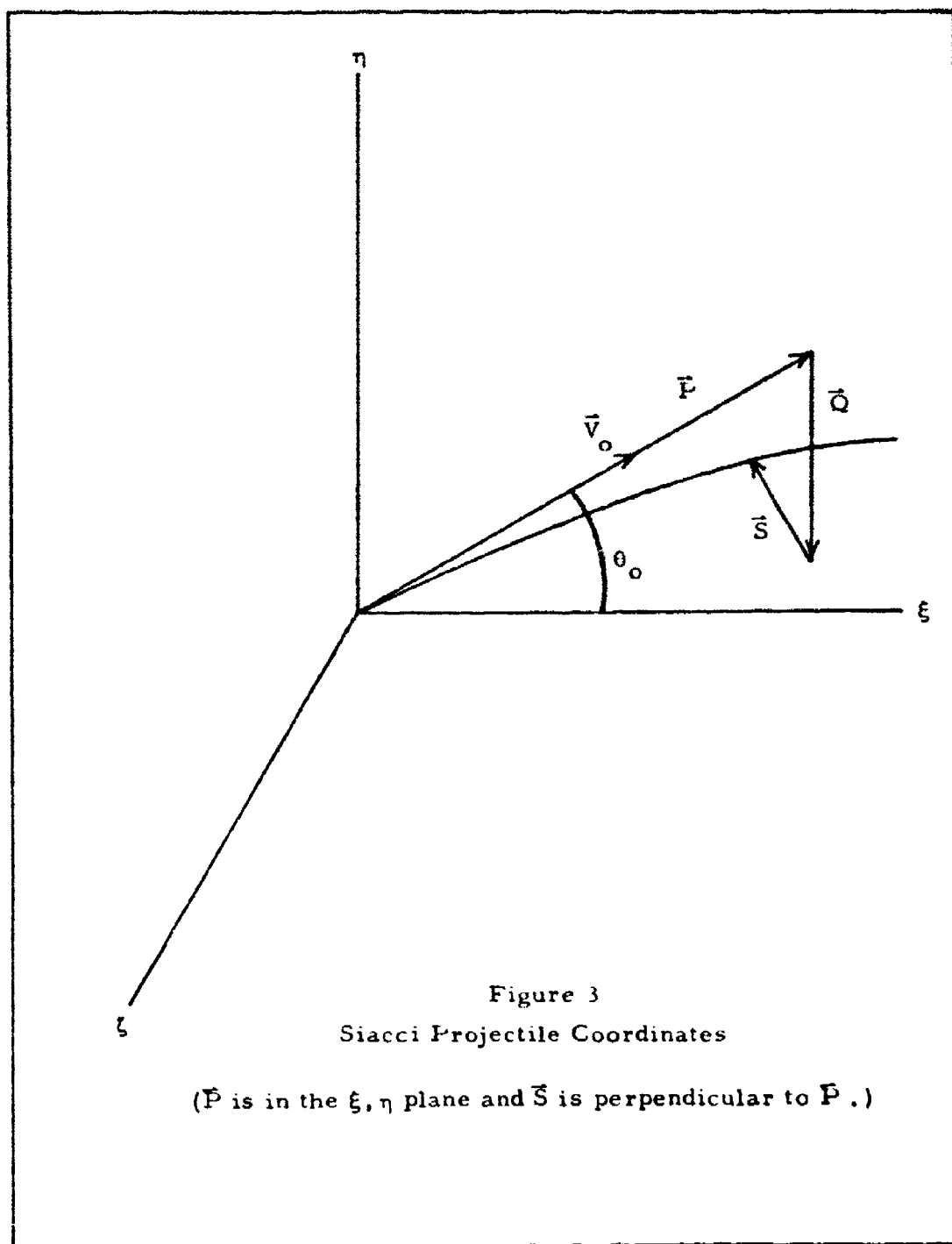
In Fig. 3, ξ, η, ζ is a right-handed coordinate system. The ξ, η plane is vertical and contains the projectile initial velocity vector $\vec{V}_o$. The ζ-axis is horizontal. The pseudorange $\vec{P}$ is along $\vec{V}_o$ and extends to a point that would be vertically above the projectile if the swerve $\vec{S}$ were zero. The gravity drop $\vec{Q}$ would be the vertical distance from the tip of $\vec{P}$ to the projectile under the same conditions. Thus, $\vec{P}$ and $\vec{Q}$ would describe the projectile trajectory if the swerve $\vec{S}$ were zero.

It follows from Fig. 3 that

$$\xi = P \cos \theta_o + S_\xi \qquad (14)$$

$$\eta = P \sin \theta_o - Q + S_\eta \qquad (15)$$

$$\zeta = S_\zeta \qquad (16)$$

where S_ξ, S_η, and S_ζ are the components of $\vec{S}$ in the ξ, η, ζ system and θ_o is the elevation angle of $\vec{V}_o$ or $\vec{P}$ above the horizontal. If these relations are substituted for the ξ, η, ζ components of Eq. (1) but with $\vec{S} = 0$, it is seen that

$$m \ddot{P} = -E_o \dot{P} \qquad (17)$$

$$m \ddot{Q} = -E_o \dot{Q} + mg \qquad (18)$$

The only difference between these equations and Eqs. (5) and (6) is the presence of E instead of E_o in Eqs. (5) and (6). But as can be seen from Eqs. (2) and (11)

$$E_o(M) = E(M, \delta = 0) \qquad (19)$$

It follows that if the time history of δ is known from some unspecified source, E could be included instead of E_o and the accuracy of Eq. (1) could be improved. Also, if $\vec{S}$ is determined by some unspecified method, a complete solution to the large-yaw problem is available. It turns out that this is possible as will be shown. It is possible to effectively delete Eqs. (7) through (10) from the set and still retain the accuracy of Eqs. (5) through (13).

13

3. The Swerve Approximation

The components of $\vec{S}$ are related to S_x and S_y by the following equations (Ref. 1)

$$S_\xi = -(S_x \cos \phi_o - S_y \sin \phi_o) \sin \theta_o \tag{20}$$

$$S_\eta = (S_x \cos \phi_o - S_y \sin \phi_o) \cos \theta_o \tag{21}$$

$$S_\zeta = S_x \sin \phi_o + S_y \cos \phi_o \tag{22}$$

where ϕ_o is the initial precession angle. Investigation of solutions of the approximate equations, i.e., Eqs. (5) through (13), shows that the windage jump components (in milliradians), namely

$$X = 10^3 S_x / P \tag{23}$$

$$Y = 10^3 S_y / P \tag{24}$$

approach constant values as the time increases, and are essentially independent of all initial conditions except initial yaw δ_o. Furthermore, it is observed that X and Y may be approximated to sufficient accuracy by the relations

$$X = a \delta_o \tag{25}$$

$$Y = b \delta_o \tag{26}$$

For the 20-mm, M56 round

$$a = 0.131 \text{ mr/deg} \tag{27}$$

$$b = 0.985 \text{ mr/deg} \tag{28}$$

when X and Y are in milliradians (mr) and δ_o is in degrees.

14

It follows that

$$\xi = P \cos \theta_o + C_\xi P \tag{29}$$

$$\eta = P \sin \theta_o - Q + C_\eta P \tag{30}$$

$$\zeta = C_\zeta P \tag{31}$$

where

$$C_\xi = -10^{-3} \delta_o (a \cos \phi_o - b \sin \phi_o) \sin \theta_o \tag{32}$$

$$C_\eta = 10^{-3} \delta_o (a \cos \phi_o - b \sin \phi_o) \cos \theta_o \tag{33}$$

$$C_\zeta = 10^{-3} \delta_o (a \sin \phi_o + b \cos \phi_o) \tag{34}$$

Thus, the swerve is given in terms of trajectory initial conditions, the pseudorange, and values of a and b calculated from a few selected trajectories obtained by means of the approximate equations of Ref. 1.

4. The Yaw-Drag Approximation

Experience has shown that the yaw-dependent drag coefficient may be written as

$$K_D(M, \delta) = K_{D_o}(M) \left[1 + K_{D_\delta 2}(M) \delta^2 \right] \tag{35}$$

There are several ways to obtain the time history of δ, but six-degree-of-freedom calculations show that it is possible to approximate δ^2 by a relation of the form

$$\delta^2 = \delta_o^2 K e^{-kP} \tag{36}$$

where K and k are constants and $K \simeq 1$. When yaw dependence is included in Eq. (1), it is seen that

$$m \frac{d\vec{V}}{dt} = - E_o \left[1 + k_o e^{-kP} \right] \vec{V} + m\vec{g} \tag{37}$$

15

where

$$k_o = K_{D_{\delta^2}} \delta_o^2 K \qquad (38)$$

Alternately, Eqs. (5) and (6) become

$$m\ddot{P} = -E_o \left[1 + k_o e^{-kP} \right] \dot{P} \qquad (39)$$

$$m\ddot{Q} = -E_o \left[1 + k_o e^{-kP} \right] \dot{Q} + mg \qquad (40)$$

In the present approximation, these last two equations, along with Eq. (12) for V, Eq. (2) for E_o, and the swerve equations of the last section, replace the entire set of approximate equations represented by Eqs. (5) through (13).

Several methods are available for acquiring values for k and K. Short of measuring δ in a spark range, the most accurate method should be to obtain yaw history data from six-degree-of-freedom calculations. Presumably, K and k do not vary much from trajectory to trajectory (i.e., for different conditions of fire) so only a few such six-degree-of-freedom calculations need be made. Yaw data obtained in this manner can be plotted on semilog paper (ln δ^2 versus P); the slope of the curve is k and the P = 0 intercept is $K\delta_o^2$.

Short of six-degree-of-freedom calculations, Eqs. (5) through (13) can be used. Alternately, the approximate equation for the yaw, Eq. (9), may be written as

$$\dot{\delta} = \frac{-\rho d^2 V}{m} \left[K_L - \frac{md^2}{A} K_T \right] \sin \delta$$

The damping term has been deleted since it is negligible. Now

$$\dot{\delta} = \frac{d\delta}{dP} \frac{dP}{dt} = u \frac{d\delta}{dP} \simeq V \frac{d\delta}{dP}$$

and if sin δ is approximated by δ, it follows that

$$\frac{d\delta}{dP} \simeq - \frac{\rho d^2}{m} \left[K_L - \frac{md^2}{A} K_T \right] \delta$$

16

Since, from Eq. (36)

$$\delta = \delta_o \sqrt{K} \ e^{-kP/2}$$

it follows that

$$\frac{d\delta}{dP} \simeq - \frac{k}{2} \ \delta_o \sqrt{K} \ e^{-kP/2} = - \frac{k}{2} \ \delta$$

and so

$$k \simeq 2 \ \frac{\rho d^2}{m} \left[K_L - \frac{md^2}{A} K_T \right] \tag{41}$$

K can be taken equal to one, or the value to be defined below by Eq. (42).

Another approach is to borrow the results of the Siacci theory as formulated by Sterne, (Refs. 5 and 6) for which the average squared yaw $\overline{\delta^2}$ is given by

$$\overline{\delta^2} = \frac{s_o - 1/2}{s_o - 1} \ \delta_o^2 \ e^{-2\sigma c P} \tag{42}$$

where s_o represents the static stability factor which is given by

$$s_o = \frac{A^2 N^2}{4B\rho d^3 V_o^2 K_M} \tag{43}$$

and

$$c = c' + \frac{c''}{s_o - 1} \tag{44}$$

where

$$c' = \frac{\rho_o d^2}{2m} \left[K_L + \frac{md^2}{B} K_H \right] \tag{45}$$

17

and

$$c'' = \frac{\rho_o d^2}{2m} K_{D_o} \tag{46}$$

B is the transverse moment of inertia of the projectile and

$$\rho_o = 0.076474 \text{ lb/ft}^3$$

is the air density at sea level.

5. The Modified Point-Mass Method

With

$$u = \dot{P}$$

and by means of

$$\frac{d}{dt}\left(\frac{\dot{Q}}{\dot{P}}\right) = \frac{\dot{P}\ddot{Q} - \ddot{P}\dot{Q}}{\dot{P}^2}$$

it can be shown that the complete set of equations to be solved is

$$m\dot{u} = -\rho d^2 V K_{D_o}\left(V/V_{sd}\right)\left[1 + k_o e^{-kP}\right]u \tag{47}$$

$$\dot{P} = u \tag{48}$$

and

$$\frac{d}{dt}\left(\frac{\dot{Q}}{u}\right) = \frac{g}{u} \tag{49}$$

where

$$V = \sqrt{\dot{P}^2 - 2\dot{P}\dot{Q}\sin\theta_o + \dot{Q}^2} \tag{50}$$

18

In many applications it has been found convenient to make the independent variable P rather than t. This is done as follows

$$\frac{du}{dt} = \frac{du}{dP} \frac{dP}{dt} = u \frac{du}{dP}$$

and hence, Eq. (47) becomes

$$m \frac{du}{dP} = - \rho d^2 V K_{D_o} \left(V/V_{sd} \right) \left[1 + k_o e^{-kP} \right] \tag{51}$$

From Eq. (48)

$$\frac{dt}{dP} = \frac{1}{u} \tag{52}$$

and from Eq. (49)

$$\frac{d}{dt} \left(\frac{\dot{Q}}{u} \right) = \left[\frac{d}{dP} \left(\frac{\dot{Q}}{u} \right) \right] \frac{dP}{dt} = u \frac{d}{dP} \left(\frac{\dot{Q}}{u} \right) = \frac{g}{u}$$

But

$$\frac{\dot{Q}}{u} = \frac{\dot{Q}}{\dot{P}} = \frac{dQ/dt}{dP/dt} = \frac{dQ}{dP}$$

and so

$$\frac{d^2 Q}{dP^2} = \frac{g}{u^2} \tag{53}$$

If we define

$$D = \frac{dQ}{dP} \tag{54}$$

it follows that

$$\frac{dD}{dP} = \frac{g}{u^2} \tag{55}$$

19

Also

$$\dot{Q} = \frac{dQ}{dP}\frac{dP}{dt} = u\frac{dQ}{dP}$$

and Eq. (50) becomes

$$V = u\sqrt{1 - 2D\sin\theta_o + D^2} \tag{56}$$

The new set of equations to be solved numerically are Eqs. (51), (52), (54), (55), and (56).

6. The Siacci Equations and Correction Terms

6.1 Basic Siacci Equations - The basic Siacci equations are also approximations to point-mass equations of motion. The method provides a closed-form solution to projectile ballistics after the tabulation of numerically integrated functions of the zero-yaw drag coefficient. The derivation of the equations has been well documented since their conception in the 1880's by F. Siacci of Italy (Refs. 2, 6, and 8). No effort will be expended here in rederivation.

The tabulated Siacci functions necessary for solution of the Siacci trajectory equations are obtained by numerical integration of the following differential equations.

$$\frac{dS}{dU} = -\frac{1}{G(U)} \tag{57}$$

$$\frac{dT}{dU} = -\frac{1}{U G(U)} \tag{58}$$

$$\frac{dI}{dU} = -\frac{g}{U^2 G(U)} \tag{59}$$

$$\frac{dA}{dU} = -\frac{I(U)}{G(U)} \tag{60}$$

where G(U) is given by

$$G(U) = \frac{U K_{D_o}(U/V_{sd})}{1883} \tag{61}$$

20

U is given by $U = u/a_o$ where u is the velocity along the initial velocity vector and a_o is the ratio of the speed of sound at the firing altitude to that at sea level. $V_{sd} = 1116.45$ ft/sec is the speed of sound at sea level for the standard atmosphere. K_{D_o} is the zero-yaw drag coefficient and $g = 32.174$ ft/sec^2 is the acceleration due to gravity. The functions S, T, I, and A are tabulated for incremental values of U. The differential equations are integrated from an arbitrary upper bound of U to an arbitrary lower bound. A tabulation of these values from U = 7,000 ft/sec to U = 500 ft/sec for the 20-mm, M56 round may be found in Ref. 9. The Siacci tables are independent of altitude, as has been shown in Refs. 2, 6, and 8.

The trajectory equations are given as follows

$$P = \frac{C}{\sigma} \left[S\left(u/a_o\right) - S\left(u_o/a_o\right) \right] \tag{62}$$

$$Q = \left(\frac{C}{\sigma a_o}\right)^2 \left[A\left(u/a_o\right) - A\left(u_o/a_o\right) - I\left(u_o/a_o\right)\frac{\sigma}{C} P \right] \tag{63}$$

$$t = \frac{C}{\sigma a_o} \left[T\left(u/a_o\right) - T\left(u_o/a_o\right) \right] \tag{64}$$

where t is the time of flight of the projectile. $\vec{P}$ is directed along the initial velocity vector $\vec{u}_o = \vec{V}_o$, $\vec{Q}$ points vertically down, and u is defined as u = dP/dt. The basic Siacci approximation to the point-mass equations of motion is that

$$V = u$$

As is evident, this approximation does not hold for extremely large values of Q. The symbol C is the ballistic coefficient and σ is the relative air density at the firing altitude.

$$C = \frac{m}{144 \, d^2} \left(\text{lb/in.}^2 \right) \tag{65}$$

where m is the mass of the round in pounds, and d is the projectile diameter in feet.

6.2 The Yaw-Drag Correction - Since the Siacci equations were derived from point-mass equations, the projectile trajectory is assumed to be in a vertical plane with no effect of yaw on the projectile drag. These assumptions are reasonably accurate for very small initial yaw angles, but corrections must be introduced for large-yaw ballistics.

According to the theory of Sterne, the yaw drag is taken into account by the approximation that the average squared yaw, $\overline{\delta^2}$, is an inverse exponential function of P given by

$$\overline{\delta^2} = \delta_o^2 \frac{s_o - 1/2}{s_o - 1} e^{-2\sigma c P} \tag{66}$$

as has been previously explained. The correction term for P, according to Sterne, is given by

$$\Delta P = - K_{D_{\delta^2}} \int_0^P \delta^2 \, dP \tag{67}$$

where δ is the yaw angle and $K_{D_{\delta^2}}$ is the yaw-drag coefficient. Combining Eqs. (66) and (67) with $\overline{\delta^2}$ substituted for δ^2 yields

$$\Delta P = - \frac{k_o}{2\sigma c} \left[1 - e^{-2\sigma c P} \right] \tag{68}$$

where

$$k_o = \frac{s_o - 1/2}{s_o - 1} K_{D_{\delta^2}} \delta_o^2 \tag{69}$$

The equation for $S(u/a_o)$ may be obtained by adding the correction term, Eq. (68), to the right-hand side of Eq. (62) and rearranging terms. In most cases, the yaw damps rapidly enough for $e^{-2\sigma c P}$ to be neglected for practical ranges. Therefore

$$S(u/a_o) = S(u_o/a_o) + \frac{\sigma}{C} P + \frac{k_o}{2c C} \tag{70}$$

22

Thus, it is apparent that if the initial conditions u_o and δ_o are known, along with the atmospheric quantities, ballistic parameters, and P, then Q and t are solved by examining the tabulated values of T, I, and A.

6.3 Curve Fit of the Siacci Functions - Storage of an extensive listing of Siacci tables is cumbersome and requires a large core-storage capacity. For this reason, the Siacci functions of the 20-mm, M56 round were curve fitted as fourth-degree polynomials. The tables were broken up into sections, and each section was curve fitted at equally spaced values of the independent variable. Reasonably good curve fit accuracy was obtained. The tables that were curve fitted are contained in Ref. 10. The curve fitting was done prior to the generation of the new tables in Ref. 9, but the two sets of Siacci tables are essentially identical.

The tabulated values of S were curve fitted as a function of U, while the values of T, I, and A were fitted as functions of S. The independent variable U extended over the range of 7,000 to 1,000 ft/sec. Though some of the trajectories computed for the comparison in Section V have a terminal velocity slightly below 1,000 ft/sec, extrapolation of the curve fits does not appear to induce severe error for the ranges considered. Caution should be exercised for ranges in excess of 5,000 ft. For longer ranges and improved accuracy, a more accurate curve fit of the tabulated values of Ref. 9 would be appropriate. The coefficients of the curve fits used in this analysis are given in Appendix I.

7. Initial Conditions

A comparison has been made between calculations done with the simplified methods described herein and those done with the approximate equations of Ref. 1. Because of the interest in air-to-ground fire-control problems at the time this work was done, air-to-ground geometry was adopted for this comparison. The equations for the necessary initial-condition computations and coordinate transformations are given in this section. The results of these calculations are given in Section IV.

It is assumed that an aircraft flies straight and level at a given altitude over a sea-level target range and that the aircraft carries a gun turret armed with an M61, 20-mm cannon. The ballistics for this round are well known (Ref. 11). The turret gimbaling is assumed to be of the depression, traverse type shown in Fig. 4. The x, y plane is horizontal and z is vertical. The aircraft flies along the x-axis, and y points out the left wing. The depression angle E is a positive rotation about the y-axis and rotates x into x'. The muzzle velocity $\overline{V}_m$ (i.e., the gun) is in the x', y plane, and A is the angle between x' and $\overline{V}_m$. Initial conditions for computations are defined by the equations below along with the transformation from the ξ, η, ζ system to the x, y, z system.
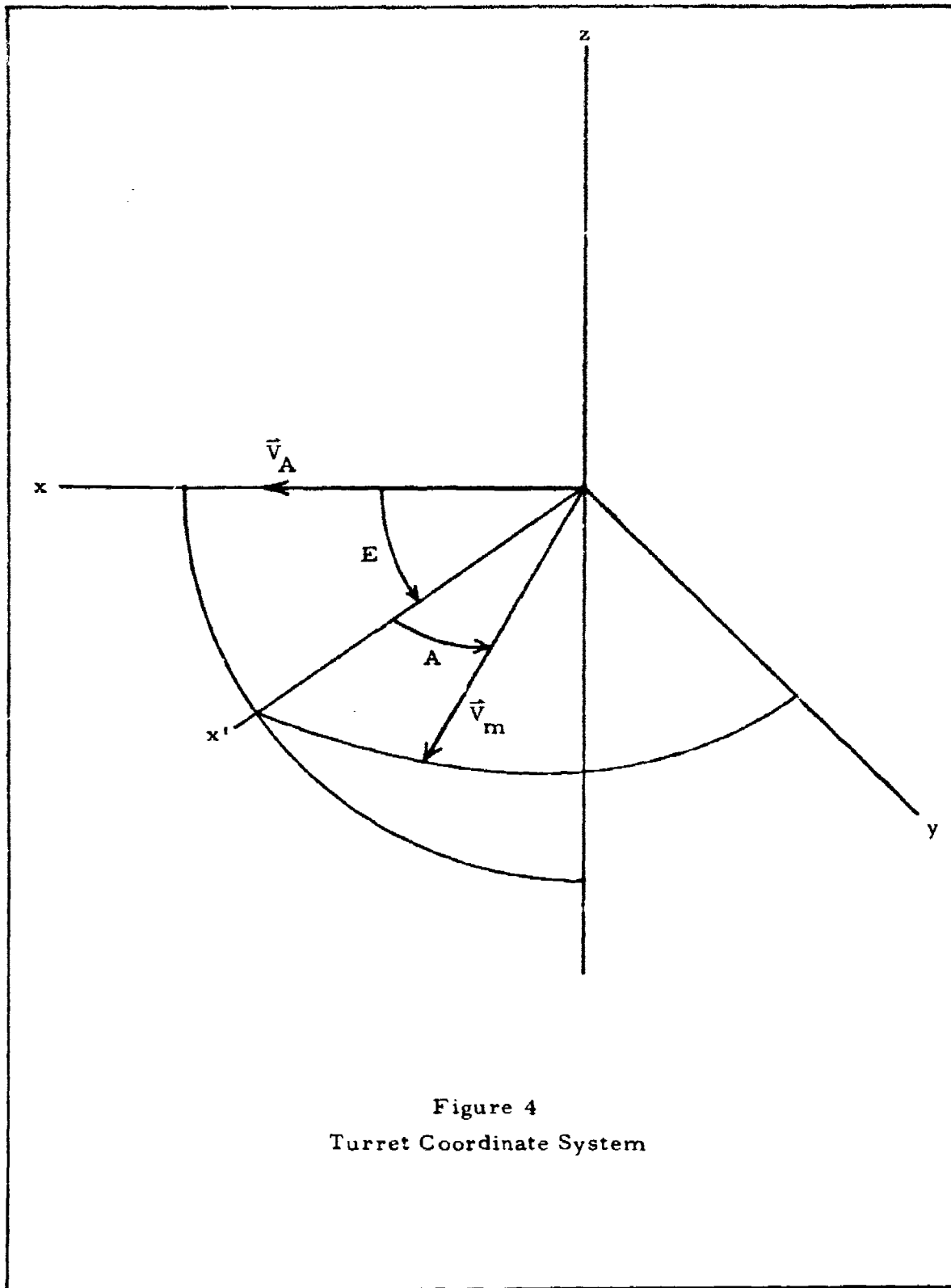
Figure 4
Turret Coordinate System

Components of $\vec{V}_o = \vec{V}_A + \vec{V}_m$ along x, y, and z are

$$V_{ox} = V_A + V_m \cos A \cos E \tag{71}$$

$$V_{oy} = V_m \sin A \tag{72}$$

$$V_{oz} = -V_m \cos A \sin E \tag{73}$$

Also

$$V_o = \sqrt{V_A^2 + 2V_A V_m \cos A \cos E + V_m^2} \tag{74}$$

and

$$\delta_o = \arccos \frac{V_m + V_A \cos A \cos E}{V_o} \tag{75}$$

The elevation angle θ_o of $\vec{V}_o$ (shown positive in Fig. 5) is defined by the equations

$$\sin \theta_o = \frac{V_{oz}}{V_o} \tag{76}$$

and

$$\cos \theta_o = \frac{V_{xy}}{V_o} \tag{77}$$

where

$$V_{xy} = \sqrt{V_{ox}^2 + V_{oy}^2} \tag{78}$$

The angle B (in Fig. 5) is defined by

$$\sin B = \frac{V_{oy}}{V_{xy}} \tag{79}$$
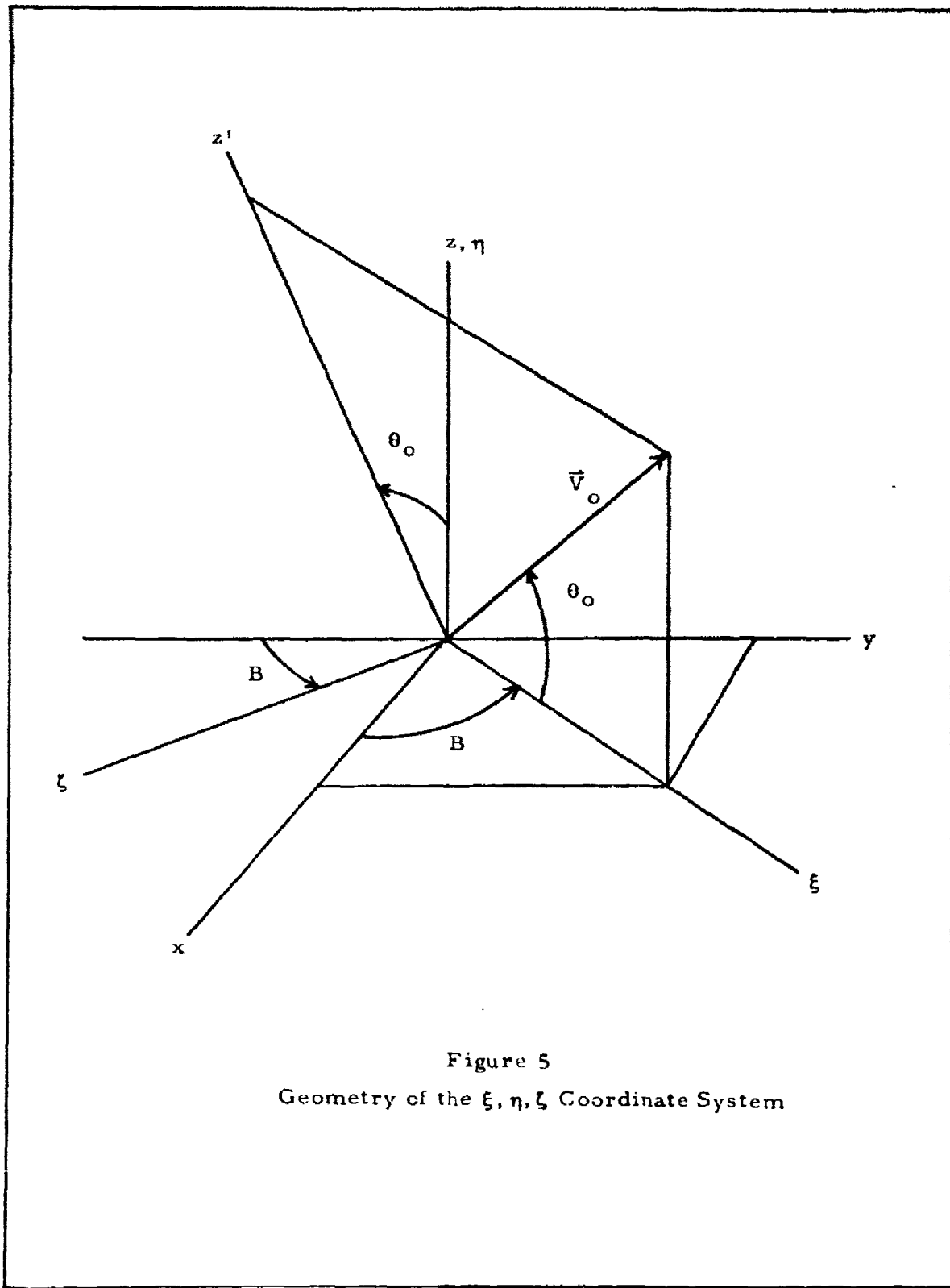
Figure 5

Geometry of the ξ, η, ζ Coordinate System

$$\cos B = \frac{V_{ox}}{V_{xy}} \tag{80}$$

The ξ, η, ζ coordinate system is defined as shown in Fig. 5. The ξ axis lies along the projection of $\vec{V}_o$ in the horizontal x, y plane, η is coincident with z, and ζ completes the right-handed set.

The initial value of the precession angle ϕ can be found by examination of Figs. 2 and 5. At time $t = 0$, the 1, 2, 3 coordinate axes of Fig. 2 lie, respectively, on the $\vec{V}_o$, z', and ζ axes of Fig. 5. Then ϕ_o is the angle between z' and the projection of $\vec{V}_m$ in the z', ζ plane. It follows that

$$\cos \phi_o = - \frac{(\cos A \cos E \cos B + \sin A \sin B) \sin \theta_o + \cos A \sin E \cos \theta_o}{\sin \delta_o} \tag{81}$$

$$\sin \phi_o = \frac{\cos A \cos E \sin B - \sin A \cos B}{\sin \delta_o} \tag{82}$$

The coordinates of a point in ξ, η, ζ transform into

$$x = \xi \cos B + \zeta \sin B \tag{83}$$

$$y = \xi \sin B - \zeta \cos B \tag{84}$$

$$z = \eta \tag{85}$$

in the x, y, z system.

In the calculations, Eq. (42) was used to define the projectile yaw history. Values used as ballistic parameters for the 20mm, M56 round are

$$c' = 0.0023 \text{ ft}^{-1}$$

$$c'' = 0.000105 \text{ ft}^{-1}$$

$$K_{D_{\delta}2} = 13.2$$

27

$$m = 0.224156 \text{ lb}$$

$$d = 0.06562 \text{ ft}$$

and

$$s_o = s_s \frac{\rho_o}{\rho} \left(\frac{V_m}{V_o}\right)^2$$

where

$$s_s = 3.5655$$

Also

$$V_m = 3300 \text{ ft/sec}$$

Values of A and B used are

$$A = 0.00013 \text{ lb-ft}^2$$

$$B = 0.00096 \text{ lb-ft}^2$$

Also

$$N = 12,1349.6 \text{ rad/sec}$$

Worst-case calculations were also done. The worst case occurs at high airspeeds when the gun is positioned so the initial yaw is maximum. As seen from Fig. 6, maximum yaw is given by

$$\sin \delta_o = \frac{V_A}{V_m}$$

when the angle between $\vec{V}_A$ and $\vec{V}_m$ is

$$E' = \delta_o + 90^o$$

It is noted that the modified point-mass calculations and the modified Siacci calculations were done at different times and the coordinate systems used in the two calculations were different. Only the coordinate system used for the modified point-mass calculations is reported herein since the two systems are equivalent and do not affect the results.
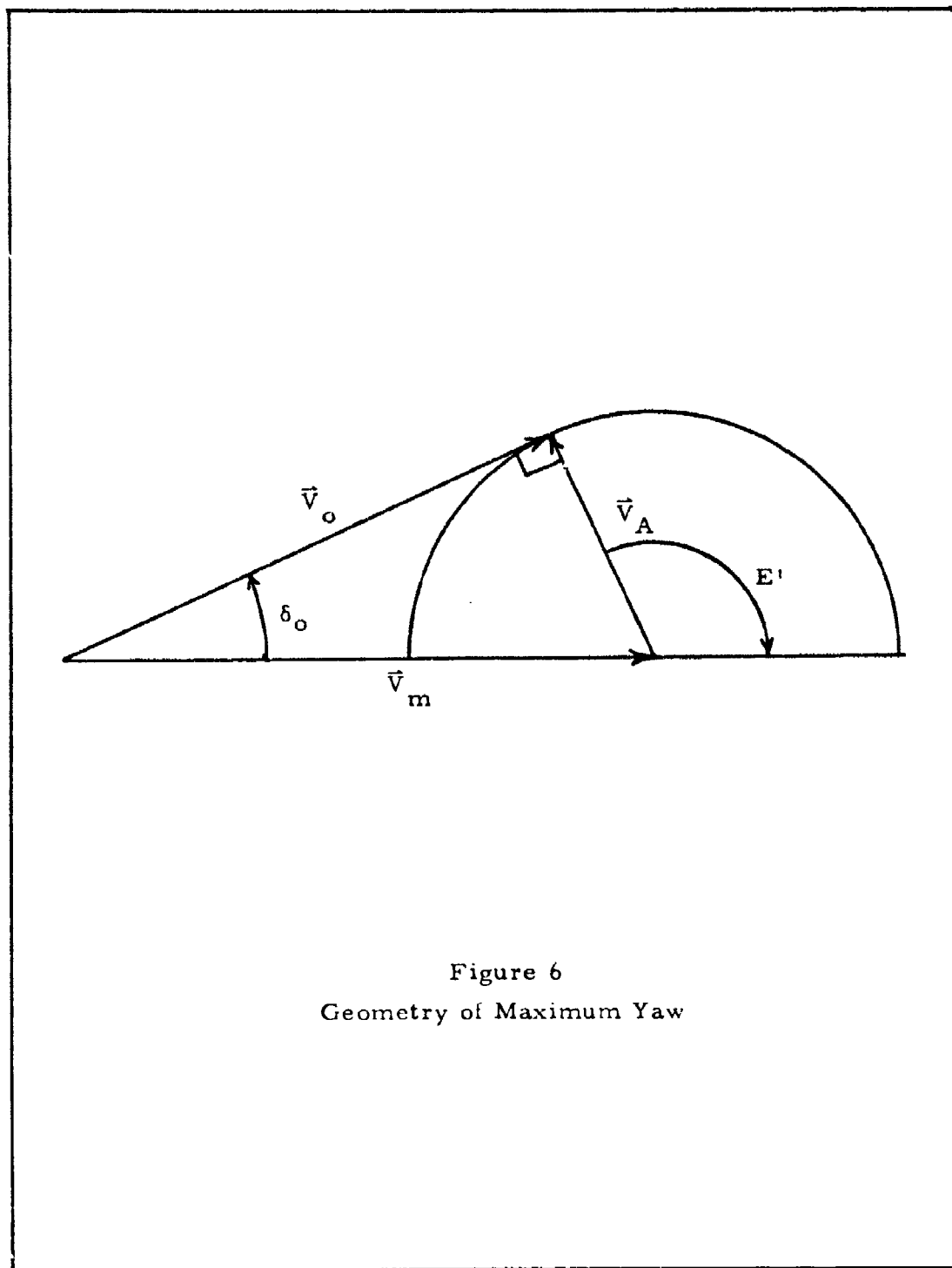
Figure 6

Geometry of Maximum Yaw

SECTION III

POLYNOMIAL CURVE FITTING OF BALLISTIC LEADS

The method presented herein for curve fitting trajectory tables has been used in the past for bombing trajectories (Ref. 12). Extension of the method to the curve fitting of firing tables is an academic matter, but must be tested to show that a high degree of accuracy may be obtained over a fairly wide range of coverage for an airborne turreted gun system. Bombing tables may generally be represented by one dependent variable, such as the trail or the spherical earth range-to-target, tabulated as a function of altitude, true airspeed, etc. Due to the necessity for a much greater delivery accuracy for gunfire, it will be necessary to curve fit at least two dependent variables, i.e., ballistic lead angles relative to the line of sight (LOS) to the target. For kinematic lead prediction and/or wind corrections, it may also be necessary to curve fit the time of flight of the projectile. The latter variable, however, will not be needed for stationary ground targets in still air, and it may be possible to approximate the time of flight to sufficient accuracy for kinematic lead prediction and/or wind corrections by means other than a polynomial curve fit.

The matrix method presented in the following sections will be studied from the standpoint of the air-to-ground situation. The target will be assumed to be stationary at sea level, the aircraft will be assumed to be flying straight and level, and it is assumed crosswind is negligible.

Four independent variables are used to curve fit the depression and deflection ballistic lead angles relative to the LOS to the target. They are relative air density, aircraft velocity, depression angle of the LOS, and deflection angle of the LOS. Aircraft altitude is extracted from the relative air density. Thus, the range to the target may be derived from the altitude and LOS angles. Two curve fits are necessary to obtain both the depression and deflection ballistic lead angles.

Equally spaced values of the independent variables are used for programming convenience. However, the derivation of the matrix equations does not contain this restriction.

The Siacci method (Refs. 2, 6, and 8) was used to generate the data to be curve fitted. Although this method is not as accurate as the numerical integration of the projectile equations of motion, it is sufficiently accurate for current exploratory computations and is much more economical. The same type of curve fits can be obtained for the more accurate ballistic data when they are needed.

1. Multidimensional Matrix Derivation for Exact Fit to the Data Points

Consider one dependent variable b and four independent variables w, x, y, and z. The values of b are known for I, J, K, and L different values of w, x, y, and z, respectively. Then, b may be expressed as a polynomial function of the independent variables and constant coefficients $A_{ijk\ell}$ as shown in Eq. (86).

$$b = \sum_{i,j,k,\ell}^{I-1,J-1,K-1,L-1} A_{ijk\ell}\; w^i x^j y^k z^\ell \tag{86}$$

The values of $A_{ijk\ell}$ must be found by use of the values of b corresponding to the various combinations of w, x, y, and z. Therefore

$$b_{pqrs} = \sum_{i,j,k,\ell}^{I-1,J-1,K-1,L-1} A_{ijk\ell}\; w^i_p x^j_q y^k_r z^\ell_s \tag{87}$$

where

$p = 0, 1, 2, ---, I-1$

$q = 0, 1, 2, ---, J-1$

$r = 0, 1, 2, ---, K-1$

$s = 0, 1, 2, ---, L-1$

In matrix form, $W = \left(W_{ip}\right)$, etc., where

$$W_{ip} = w^i_p, \text{ etc.}$$

Define the inverse of the independent variable matrices as follows

$$C = W^{-1}, \; D = X^{-1}, \; E = Y^{-1}, \; F = Z^{-1}$$

so that

$$\sum_p W_{ip} C_{pa} = \delta_{ia}$$

$$\sum_q X_{jq} D_{qb} = \delta_{jb}$$

$$\sum_r Y_{kr} E_{rc} = \delta_{kc} \tag{88}$$

$$\sum_s Z_{\ell s} F_{sd} = \delta_{\ell d}$$

Thus

$$\sum_{p, q, r, s} b_{pqrs} C_{pa} D_{qb} E_{rc} F_{sd}$$

$$= \sum_{i, j, k, \ell} A_{ijk\ell} \, \delta_{ia} \, \delta_{jb} \, \delta_{kc} \, \delta_{\ell d} \tag{89}$$

The δ terms are elements of the identity matrices; hence

$$A_{abcd} = \sum_{p, q, r, s} b_{pqrs} W_{pa}^{-1} X_{qb}^{-1} Y_{ec}^{-1} Z_{sd}^{-1} \tag{90}$$

Equation (90) is the symbolic form of the general coefficient matrix and may be easily expanded to N-dimensions by inspection. Substitution of Eq. (90) into Eq. (86) along with specific values of the independent variables yields the desired dependent variable.

Normalizing the independent variable matrices will simplify the matrix algebra and reduce round-off error acquired in matrix inversion.

32

Suppose the independent variables are σ (relative air density), V_A (aircraft velocity), A_T (LOS deflection to target) and E_T (LOS depression to target). $\Delta\sigma$, ΔV_A, ΔA_T, and ΔE_T are equal intervals between successive variations in the independent variables. The subscript m indicates the value of the variable at the mid-point of the region covered by each variable. The normalized variables used in the curve fit are then defined as follows

$$w = \frac{\sigma - \sigma_m}{\Delta\sigma}$$

$$x = \frac{V_A - V_{Am}}{\Delta V_A}$$

$$y = \frac{A_T - A_{Tm}}{\Delta A_T} \tag{91}$$

$$z = \frac{E_T - E_{Tm}}{\Delta E_{Tm}}$$

The matrices W, X, Y, and Z will be of the form

$$
W = \begin{bmatrix}
1 & 1 & \cdot & \cdot & \cdot & \cdot & 1 \\
w_0 & w_1 & \cdot & \cdot & \cdot & \cdot & w_{I-1} \\
w_0^2 & w_1^2 & \cdot & \cdot & \cdot & \cdot & w_{I-1}^2 \\
\cdot & \cdot & & & & & \cdot \\
\cdot & \cdot & & & & & \cdot \\
\cdot & \cdot & & & & & \cdot \\
w_0^{I-1} & w_1^{I-1} & \cdot & \cdot & \cdot & & w_{I-1}^{I-1}
\end{bmatrix} \tag{92}
$$

The order of matrix (92) is equal to the number of data points and will depend upon the degree of the polynomial. The polynomial $b(w,x,y,z)$ is of degree I-1 in w. Hence, I data points are required and the order of W is I. The W matrix is shown in Eqs. (93) through (96) for I = 2, 3, 4, and 5.

For I = 2

$$W = \begin{bmatrix} 1 & 1 \\ -0.5 & 0.5 \end{bmatrix} \tag{93}$$

For I = 3

$$W = \begin{bmatrix} 1 & 1 & 1 \\ -1 & 0 & 1 \\ 1 & 0 & 1 \end{bmatrix} \tag{94}$$

For I = 4

$$W = \begin{bmatrix} 1 & 1 & 1 & 1 \\ -1.5 & -0.5 & 0.5 & 1.5 \\ 2.25 & 0.25 & 0.25 & 2.25 \\ -3.375 & -0.125 & 0.125 & 3.375 \end{bmatrix} \tag{95}$$

and for I = 5

$$W = \begin{bmatrix} 1 & 1 & 1 & 1 & 1 \\ -2 & -1 & 0 & 1 & 2 \\ 4 & 1 & 0 & 1 & 4 \\ -8 & -1 & 0 & 1 & 8 \\ 16 & 1 & 0 & 1 & 16 \end{bmatrix} \tag{96}$$

It may also be necessary to normalize the dependent variable to reduce errors associated with round off. If a_m is the value of the dependent variable a when the independent variables are σ_m, V_{Gm}, A_{Tm}, and E_{Tm}, and N_a is a normalizing constant which may be chosen to reduce the values of the dependent variables to near unity, the dependent variable to be curve fitted is taken to be

$$b = \frac{a - a_m}{N_a} \tag{97}$$

If the values of a are not excessively large or small, $N_a = 1$ will be adequate.

2. Programming and Storage for the N-Dimensional Arrays

Since both b and A are multidimensional arrays, it is convenient to store their values in a linear array fashion (our CDC 3200 computer cannot handle four-dimensional arrays with the currently used FORTRAN IV system). The following sample program should serve to relax programming complexity which occurs when the multidimensional equations are broken up into two-dimensional matrix algebra.

It is assumed that the variables have been normalized, and the values of the dependent variable at equal intervals are given. The coefficient matrix can be obtained by use of the following program.

```
      PROGRAM CURVEFIT

C     4-DIMENSIONAL CURVE FIT

C     INDEPENDENT VARIABLES X1, X2, X3, X4

C     DEPENDENT VARIABLE Z

C     COEFFICIENT MATRIX A

C     NUMBER OF DATA POINTS FOR EACH VARIABLE

C     RESPECTIVELY, I, J, K, L

      DIMENSION Z(625), X1(5,5), X2(5,5), X3(5,5), X4(5,5), A(625)

      READ 10, I, J, K, L
```

```
10  FORMAT (4I1)

    READ 20, ((X1(N,M), M = 1,I), N = 1,I)

    READ 20, ((X2(N,M), M = 1,J), N = 1,J)

    READ 20, ((X3(N,M), M = 1,K), N = 1,K)

    READ 20, ((X4(N,M), M = 1,L), N = 1,L)

20  FORMAT (10F8.1)

    KL = I*J*L*K

    READ 20, (Z(N), N = 1, KL)
C       SUBROUTINE INVERT (X) INVERTS X.  THE X ARRAY STORAGE
C       IS USED FOR STORAGE OF THE INVERSE
    CALL INVERT (X1)

    CALL INVERT (X2)

    CALL INVERT (X3)

    CALL INVERT (X4)

    DO 40 II = 1,I

    DO 40 JJ = 1,J

    DO 40 KK = 1,K

    DO 40 LL = 1,L

    N = (II-1)*J*K*L + (JJ-1)*K*L + (KK-1)*L + LL

    A(N) = 0.

    DO 30 IP = 1,I

    DO 30 IQ = 1,J

    DO 30 IR = 1,K

    DO 30 IS = 1,L
```

$$M = (IP-1)*J*K*L + (IQ-1)*K*L + (IR-1)*L+IS$$

$$A(N) = A(N) + Z(M)*X1(IP,II)*X2(IQ,JJ)*X3(IR,KK)$$

$$*X4(IS,LL)$$

30 CONTINUE

40 CONTINUE

PUNCH 50, (A(N), N = 1, KL)

50 FORMAT (4E20.12)

END

It should be noted that the X matrices should be read in by varying columns and then rows. The values of the dependent variable Z_{ijkl} should be read in while varying the parameters in reverse order, i.e., l, k, j, and i. The output of matrix A will, therefore, be in the same order as Z was input. Although the program was set up for 4-dimensional curve fit with a maximum of five data points for each independent variable, it may be easily expanded to a higher-degree fit by insertion of the required parameters and an increase in the size of the dimensioned arrays.

3. Evaluation of the Accuracy of the Curve Fit for Air-to-Ground Fire of a 20-mm Gun

To determine the range through which the independent variables may be varied and to what degree they must be curve fit, it is necessary to estimate the degree of each variable and test the curve fits at points between the mesh of data points. This leads to a trial-and-error sequence in which an effort is made to optimize the curve fit for a pre-specified accuracy. Any desired accuracy may be obtained by decreasing the range of coverage and/or increasing the degree of the curve fit. The problem then, is one of attempting to minimize the number of curve-fit coefficients necessary to describe all of the ballistic lead angles within the effective coverage of the gun system.

A turreted, 20-mm gun was selected for a quantitative evaluation of the curve-fit method because of the availability of the ballistic data necessary for trajectory calculations. The Siacci method was used to determine the lead angles to be curve fit, rather than numerical integration of the equations of motion, to reduce the computation time required.

37

Coordinate systems are defined as follows: In Figs. 7 and 8, the x, y, z coordinate system is earth fixed with x and z horizontal and y vertical. The angle B is rotated clockwise about the y-axis, and is measured between the x-axis and the ξ-axis. The ξ-axis lies along the projection of the vector $\vec{u}_o$ in the horizontal plane. The η-axis is co-incident with the y-axis and the ζ-axis completes a right-hand ξ, η, ζ system. The angle θ_o is measured between $\vec{u}_o$ and the ξ-axis. The vectors $\vec{V}_m$, $\vec{V}_A$, and $\vec{u}_o$ are, respectively, the projectile muzzle velocity, the aircraft velocity, and the projectile initial velocity, where

$$\vec{u}_o = \vec{V}_m + \vec{V}_A$$

In Fig. 7, E_G is the depression angle of the gun measured between the x-axis and the projection of $\vec{V}_m$ on the x, y plane. A_G, the deflection angle of the gun, is the angle between $\vec{V}_m$ and the x, y plane.

In Fig. 8, A_Z and E_L are the azimuth and elevation angles of the gun, respectively. A_Z is measured between the projection of $\vec{V}_m$ in the x, z plane and the x-axis, and E_L is measured between $\vec{V}_m$ and the x, z plane.

First, the azimuth-elevation system (Fig. 8) was used for the gun pointing angles, but some difficulty arose in the curve fitting of the azimuth lead angle. A fourth-order curve fit in all four variables produced errors that were generally less than 1 mr, but were as high as 10 mr at some points on the curve fit. The relative air density was varied from 0.98 to 0.86 (approximately 700 to 5000 ft in altitude) while the aircraft velocity, azimuth LOS angle, and elevation LOS angle, respectively, were varied; (200 to 500 ft/sec), (0 to 120 deg, and (-45 to -75 deg).

In an effort to decrease the maximum error of the azimuth curve fit, gun lead angles were changed to the depression-deflection system (Fig. 7). This angular arrangement proved to be considerably easier to fit and corresponds to a more natural gimbal system for a turreted air-to-ground gun. The angular coverage in depression angle E_G, and deflection angle A_G, are, respectively, -30 to -135 deg and -30 to 30 deg. The aircraft velocity ranged between 200 and 800 ft/sec, and the relative air density between 0.98 and 0.86.

Figures 9, 10, 11, and 12 represent plots of the depression and deflection lead angles vs target LOS angles as calculated by the Siacci
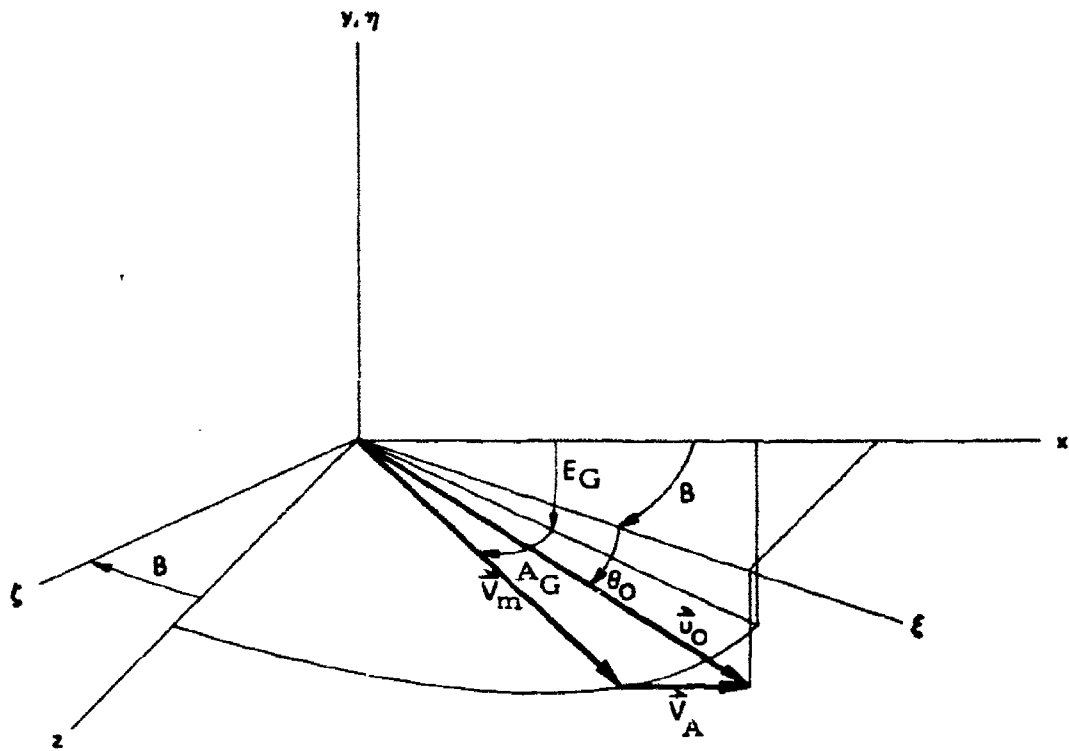
Figure 7

Depression - Deflection System
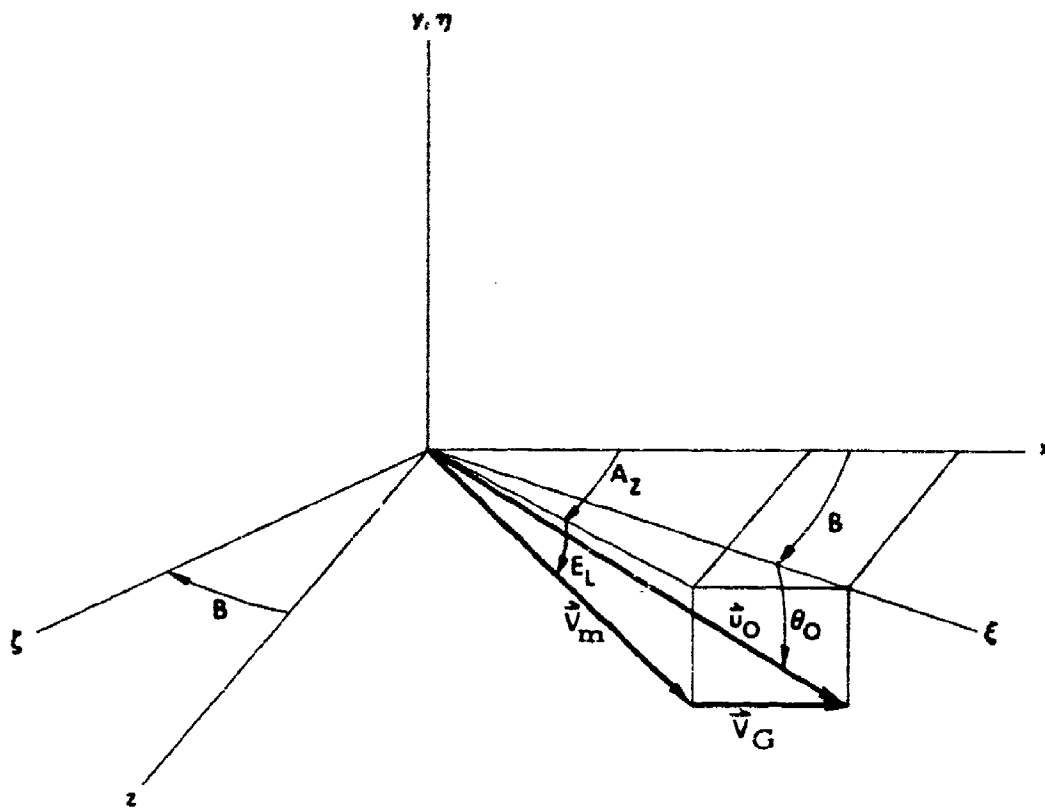
Figure 8
Azimuth-Elevation System

40
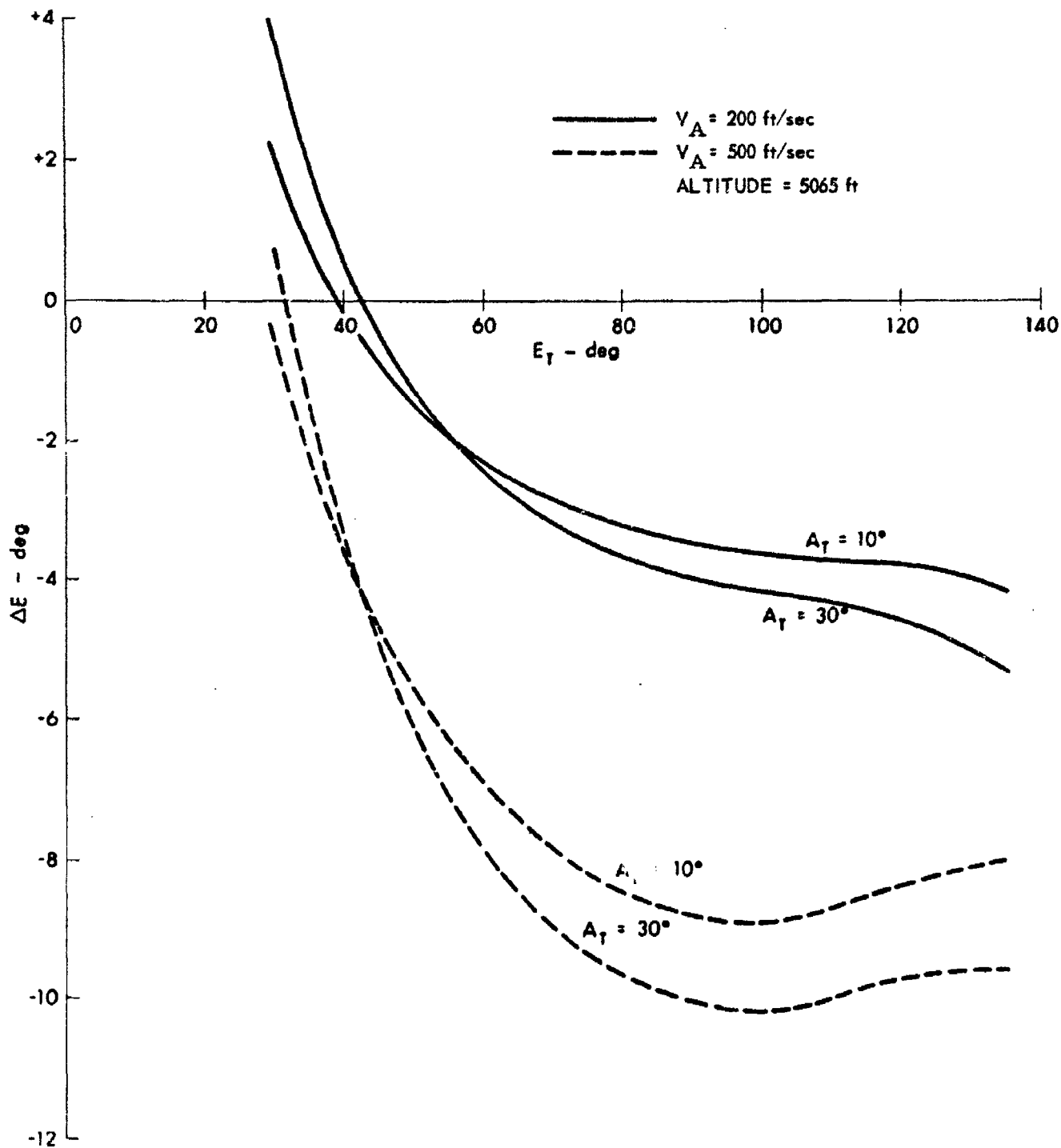
Figure 9

Depression Lead Angle
vs LOS Depression to Target
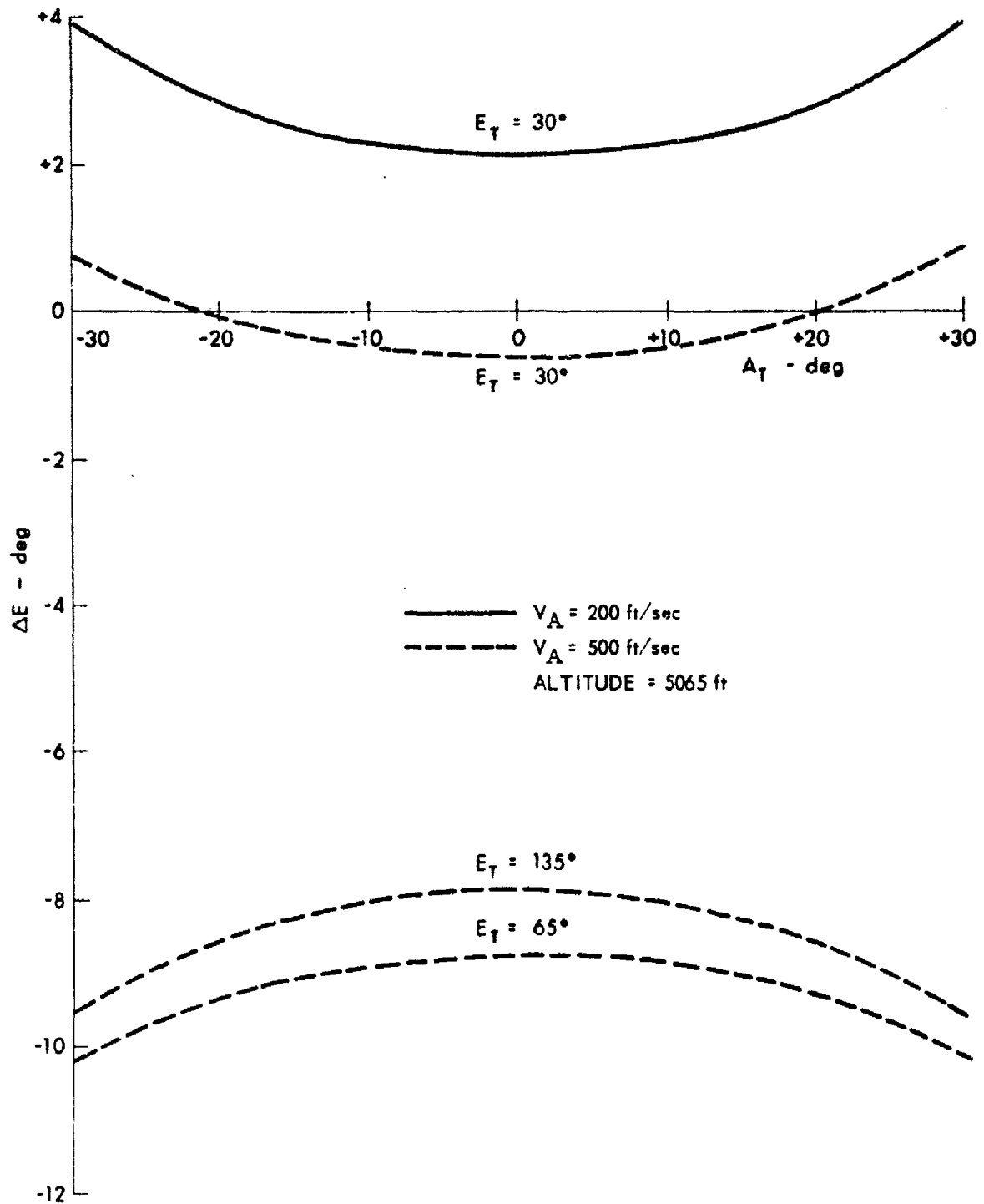
Figure 10

Depression Lead Angle
vs LOS Deflection to Target
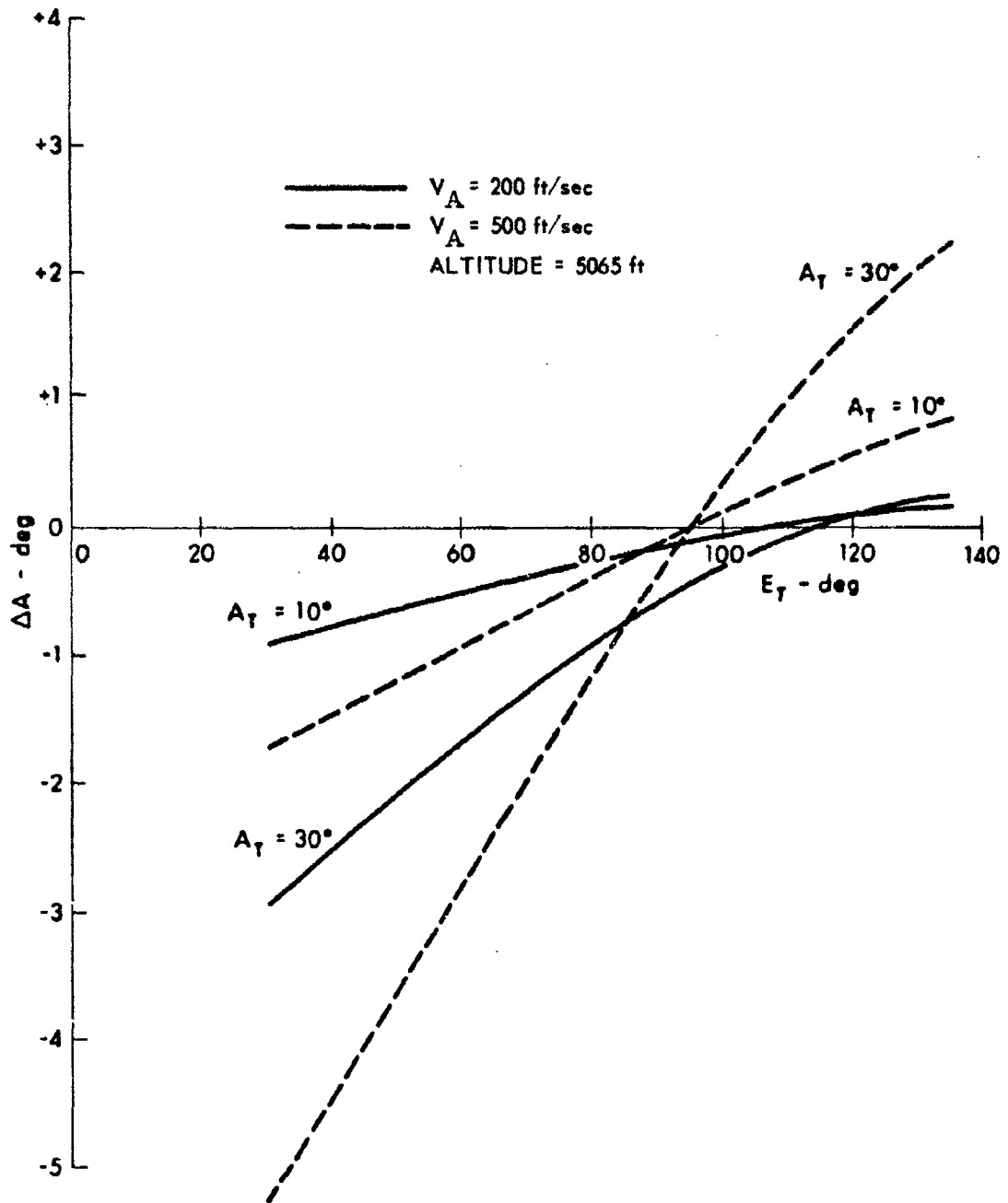
Figure 11

Deflection Lead Angle vs LOS
Depression to Target

43
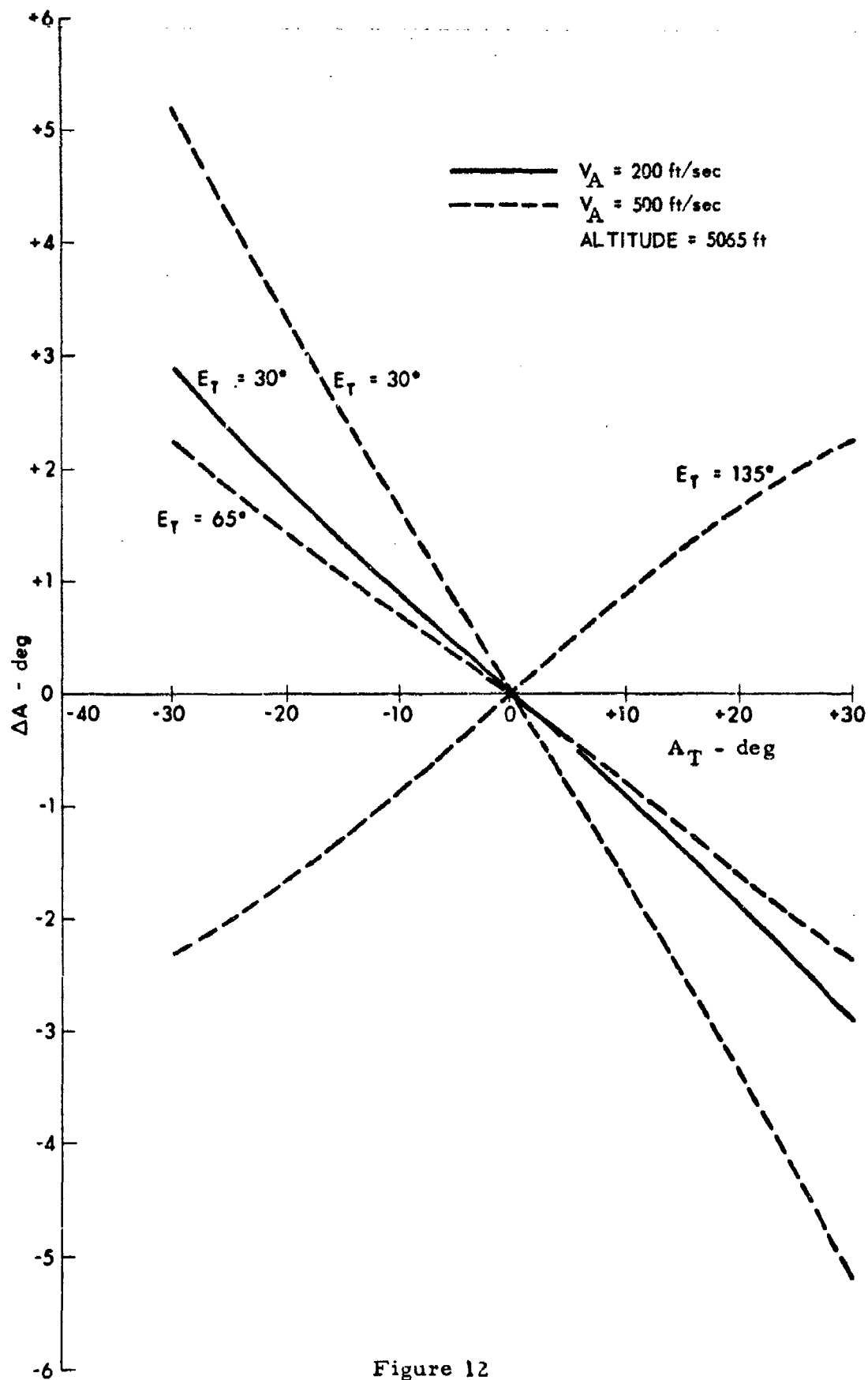
Figure 12
Deflection Lead Angle vs LOS
Deflection to Target

44

method. These plots were used to aid in the first estimate of the degree of the polynomial required for the two independent variables A_T (LOS deflection to target) and E_T (LOS depression to target). Figure 9 suggests that ΔE (depression lead) may be approximated by a fifth-degree polynomial in E_T. The accuracy of the curve fit is arbitrary, but directly affects the number of coefficients required. A convenient tolerance of ±2 mr was selected, well within the gun pointing accuracy of current airborne fire-control systems. The original computer code was set up for computation of the coefficients for a polynomial of no higher than fourth-degree in any of the independent variables. After several unsuccessful attempts to obtain fourth-degree curve-fit accuracy with a ±2 mr tolerance for ΔE over the entire range of E_T, A_T, σ, and V_A, the curve fit was separated into two regions. The variable E_T ranged between 30 and 90 deg in the first region, and between 90 and 135 deg in the second region. The remaining three variables extended over their entire range in both regions of the curve fit. After examination of Figs. 10, 11, and 12, and some trial-and-error experimentation, it was found that a good curve fit could be obtained with variables of the following degrees: $\Delta E \{ \sigma(2), V_A(2), A_T(3), E_T(4) \}$ over two regions, and $\Delta A \{ \sigma(2), V_A(2), A_T(3), E_T(3) \}$. The variable ΔA required only one curve fit. The number of data points required for each independent variable is equal to the degree plus one. Therefore, each section of ΔE required $3 \times 3 \times 4 \times 5 = 180$ points, and ΔA required $3 \times 3 \times 4 \times 4 = 144$ points for a total of $2 \times 180 + 144 = 504$ points. This is also the total number of coefficients in the polynomial curve fits.

4. Comparison of the Siacci Curve Fit With 20-mm, Large-Yaw Trajectory Tables

This section contains a comparison of the Siacci method of ballistic computation with the approximate equations of motion of Ref. 1. (Also, see Section IV of this report.) The approximate equations were used in the computation of M56, 20-mm trajectory tables compiled by the Air Force Armament Laboratory (Ref. 13). The purpose of the comparison is not to show that the Siacci method is a highly accurate means of performing ballistic computations for large-yaw, long-range trajectories, but rather, to show that the curve fit of the Siacci data could be used for limited angular coverage and limited range for onboard ballistic lead computation. A more realistic approach, however, is to curve fit the lead angles obtained from the approximate equations of motion or any other method which is better suited to large-yaw ballistic computations. This is not done here because of the relatively lengthy time required for ballistic lead computation by methods requiring small step-size, numerical integration.

Selected trajectories in the firing tables (Ref. 13) were used for comparison with the Siacci curve fit. The three components of range to the target in the tables were used to resolve the LOS angles. The leads were then computed by subtracting the gun angles from the LOS angles. Contrary to the firing tables, the depression angle for the curve fit is considered positive when below the horizontal.

The table in Appendix III contains a complete list of the depression and deflection lead angles as obtained from both the Siacci curve fit and the firing tables. Comparison was made between the lead angles for gun depression angles of 45, 65, 85, and 105 deg. Reasonable agreement was obtained for the smaller depression angles, but for 105 deg there was a large deviation between Siacci calculations and the firing tables. This may be due to round-off error in the firing tables at near 90 deg depression angles or computational errors in the direction-cosines for an initial velocity vector depression angle greater than 90 deg. Only data for the smaller depression angles will be considered. Figures 13 and 14 are plots of the difference between Siacci calculations and the firing tables. It should be noted that a biased deviation between the two methods may be essentially eliminated by adjustment of the ballistic coefficient used in the Siacci calculations, or by adjusting the first coefficient of the curve fit. By simple inspection of the graphs, it appears that an average deviation for both the depression and deflection lead angles is approximately ±0.5 deg (±8.7 mr) with the bias removed.

The results of this section should be compared with those of Section IV where Siacci computations are also compared with results of calculations using the approximate equations of motion of Ref. 1. In both instances, the same set of approximate equations was used. In this section, the difference between leads calculated by use of the two methods may be as much as 1 deg, whereas the difference indicated in Section IV is usually less than 1 mr. The suspected reason for this discrepancy will be discussed in Section IV.

5. Variables not Included in the 4-D Curve Fit

The four-dimensional curve fit presented here is complete only if we assume straight-and-level flight, a sea-level target, and wind and atmospheric deviations from standard are negligible. The flight altitude and target altitude may be accurately taken into account by increasing the number of independent variables in the curve fit or by curve fitting for several target altitudes and interpolating for points between curve fits. Alternately, consider the following argument. Near sea level, the air density ρ is approximately given by

$$\rho(z) = \rho_0 e^{-hy}$$

46
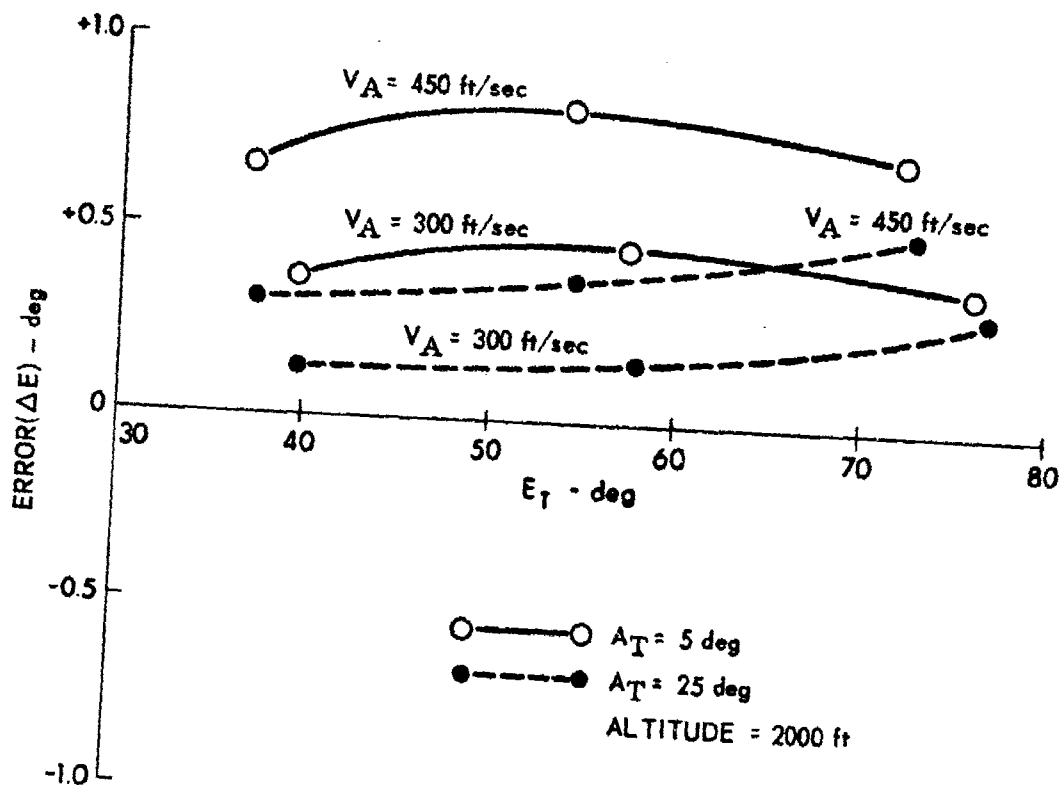
Figure 13
Difference Between the Depression Lead Angle
Curve Fit and the Firing Tables
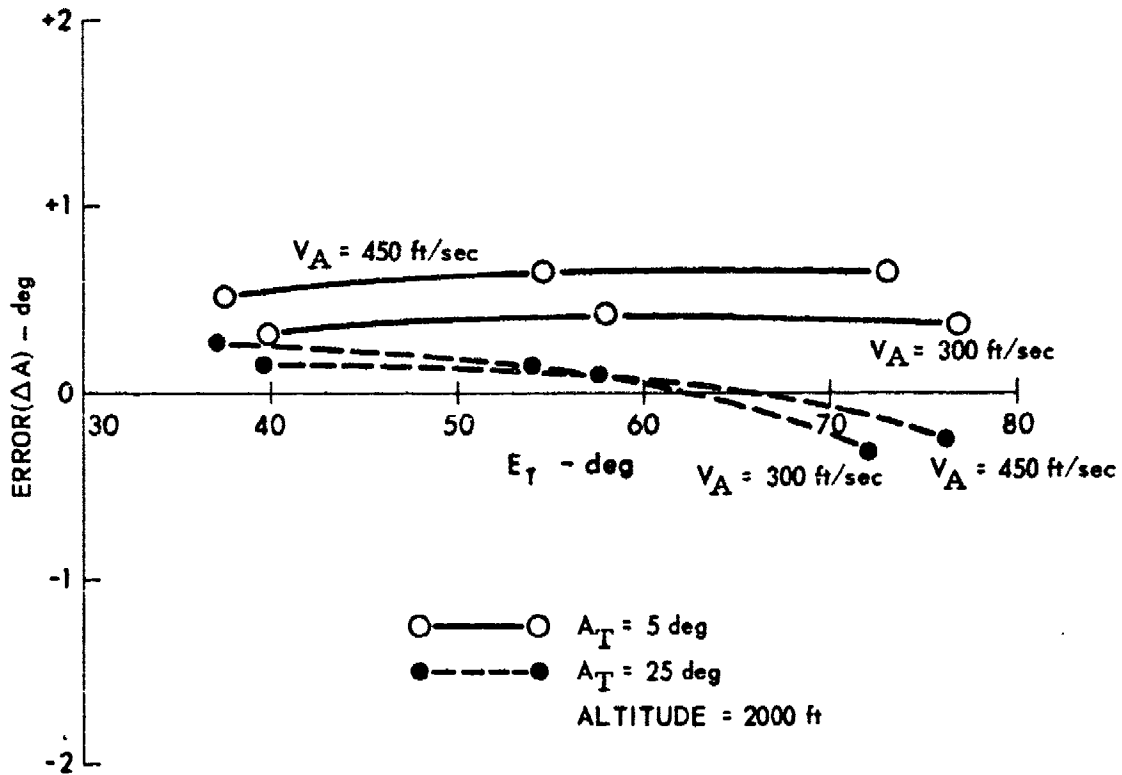
Figure 14

Difference Between the Deflection Lead Angle
Curve Fit and the Firing Tables

48

where ρ_o is sea-level air density, y is altitude above sea level, and h is a constant. If y_T is target altitude and y_A is aircraft altitude, the relative air density between the aircraft and the target is

$$\frac{\rho(y_A)}{\rho(y_T)} = \frac{\rho_o e^{-hy_A}}{\rho_o e^{-hy_T}} = e^{-h(y_A - y_T)}$$

But, this is the same as

$$\frac{\rho(y_A - y_T)}{\rho_o} = e^{-h(y_A - y_T)}$$

Use of

$$\sigma = \frac{\rho(y_A)}{\rho(y_T)}$$

in the curve fits should be accurate enough for most purposes since $\rho(y)$ does not change much over a few hundred feet. The curve fits given here are for targets at or near sea level. Curve fits for combat zones at higher altitudes can easily be obtained.

For most air-to-ground applications, the only parameter needed in addition to the ones listed above would be the dive angle. As necessary, any other attitude parameters could be treated by means of appropriate coordinate transformations. Effects of wind and atmospheric deviations can probably be handled by some form of differential corrections to lead angles. In most cases, however, these effects will be small and, possibly, negligible.

SECTION IV

SUMMARY AND CONCLUSIONS

1. Modified Point-Mass Method

A new, simplified set of approximate, large-yaw, ballistic tra-
jectory equations has been developed which are in excellent agreement
with the set of approximate equations used at Eglin Air Force Base to
generate trajectory tables. When the new, simplified set of equations is
used, a reduction in computer time by a factor (depending on firing
geometry) of 15 to 20 over the old set can be expected. This new set of
equations is almost as simple as the particle trajectory equations used
in the F-111D Mk II avionics system package and is a candidate set for
airborne calculations in some applications.

A comparison has been made between computations done with the
simplified method described herein and those done with the approximate
equations used at Eglin AFB (Ref. 1). The results of these calculations
are summarized in Tables I, II, and III for three aircraft altitudes,
2000 ft, 5000 ft, and 8000 ft, respectively. Calculations were done for
three values of aircraft velocity V_A (200 knots, 300 knots, and 400 knots)
and two values of gun traverse angle A (0° and 30°). Three values of gun
depression angle E (30°, 60°, and 90°) appear in Tables I and II and two
values (60° and 90°) appear in Table III. The initial yaw angle δ_o, the
projectile time of flight, and the range from the gun to the target are
tabulated for each trajectory.

Coordinates ξ and ζ represent the projectile impact point on the
ground (at sea level) as calculated with the old approximate method, and
$\Delta\xi$ and $\Delta\zeta$ represent the amount by which calculations done with the new
simplified method differ from those done with the old method (old minus sim-
plified). As seen by the pilot (Fig. 15), ξ is measured downrange on the ground
along the projection of $\vec{V}_o$ (the initial projectile velocity vector) in the
horizontal plane, and ζ is measured to the right. The radial difference
is the square root of the sum of the squares of $\Delta\xi$ and $\Delta\zeta$. Agreement
between the two methods is excellent. It is doubtful that the old approxi-
mate calculational method compares with actual measured trajectories as
well as these two calculations agree.

Worst-case calculations were also done. The worst case occurs
for high aircraft velocities when the gun is positioned so the initial pro-
jectile yaw (angle of attack) is maximum. Maximum yaw occurs when
$\vec{V}_o = \vec{V}_m + \vec{V}_A$ is perpendicular to $\vec{V}_A$, e.g., for straight-down fire.
Computations were done for altitudes of 2000 ft, 5000 ft, and 8000 ft with
an airspeed V_A of 600 knots (just under Mach 1), a traverse angle A of 0 deg,
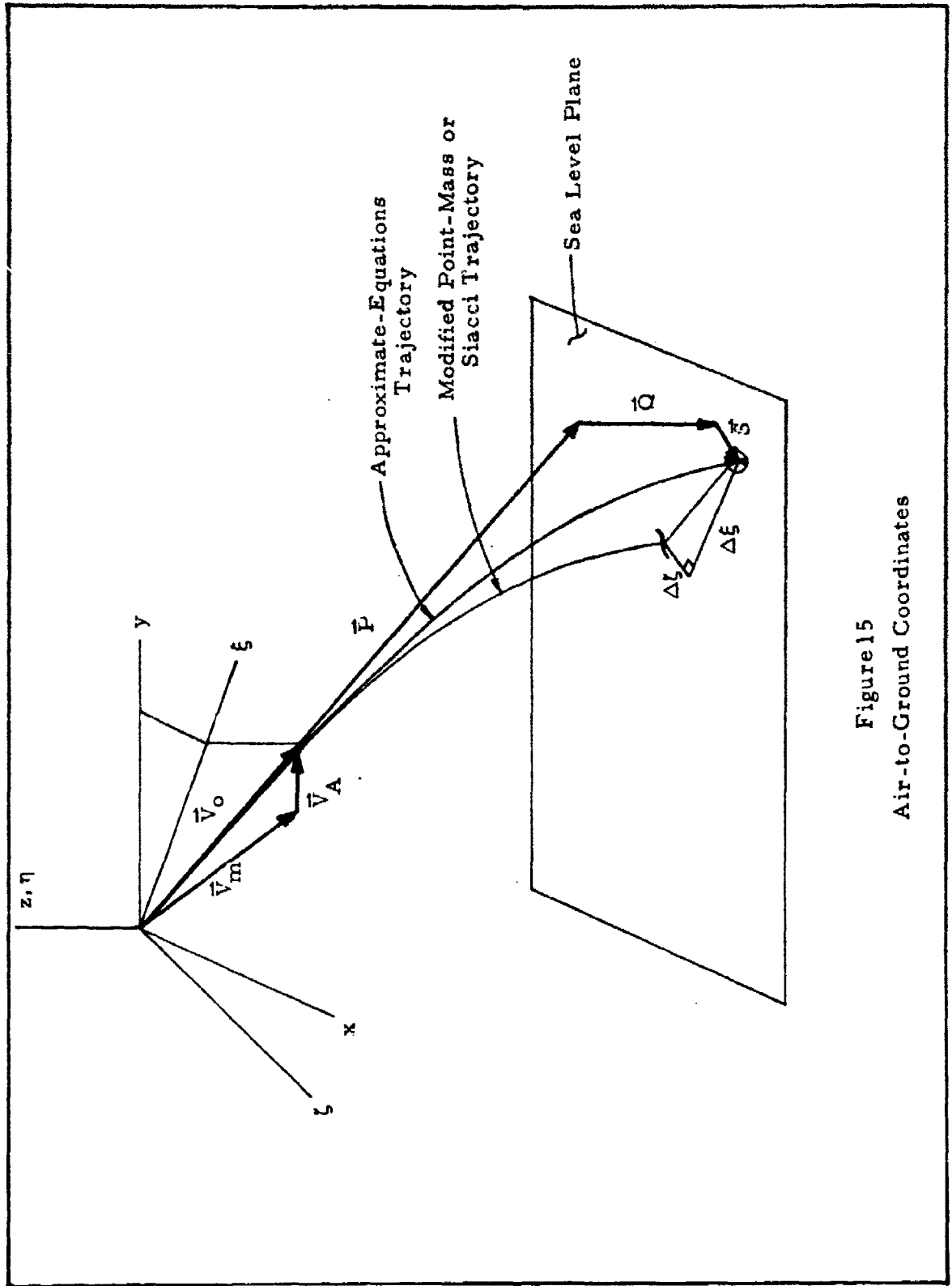
Figure 15
Air-to-Ground Coordinates

51

Table I

Comparison Between the Simplified Approximate Theory and the Old Approximate Theory for a Gun Altitude of 2000 ft

V_A (knots)	E (deg)	A (deg)	Initial Yaw (deg)	Time of Flight (sec)	Range to Target (ft)	ξ (ft)	$\Delta\xi$ (ft)	ζ (ft)	$\Delta\zeta$ (ft)	Radial Difference (ft)
200	30	0	2.69	2.04	4275	3778.2	0.1	-10.6	0.7	0.7
		30	3.60	2.54	4802	4366.3	2.0	-7.3	0.4	2.0
	60	0	4.82	0.92	2431	1381.8	0.1	-10.9	0.6	0.6
		30	5.05	1.11	2774	1922.0	0.9	-6.6	0.3	0.9
	90	0	5.84	0.76	2010	203.0	0.2	-10.9	0.6	0.6
		30	5.84	0.91	2311	1157.2	0.9	-0.6	0.0	0.9
300	30	0	3.87	2.07	4449	3973.6	0.1	-16.4	0.5	0.5
		30	5.20	2.57	4961	4540.2	1.8	-11.3	0.4	1.8
	60	0	7.04	0.93	2499	1498.0	0.0	-17.0	0.2	0.2
		30	7.39	1.12	2838	2013.7	0.4	-10.8	0.1	0.4
	90	0	8.72	0.77	2023	304.0	0.1	-17.2	0.1	0.1
		30	8.72	0.92	2321	1177.8	0.2	-2.6	-0.1	0.2
400	30	0	4.97	2.10	4623	4168.1	-0.5	-22.5	0.0	0.5
		30	6.69	2.60	5120	4713.6	0.1	-15.6	0.2	0.2
	60	0	9.13	0.94	2570	1614.0	-0.1	-23.6	-0.6	0.6
		30	9.62	1.13	2906	2108.2	-0.8	-15.6	-0.4	0.9
	90	0	11.56	0.78	2041	404.9	0.0	-24.4	-1.3	1.3
		30	11.56	0.93	2336	1207.9	-1.5	-5.9	-0.5	1.6

Table II

Comparison Between the Simplified Approximate Theory and the Old Approximate
Theory for a Gun Altitude of 5000 ft

V_A (knots)	E (deg)	A (deg)	Initial Yaw (deg)	Time of Flight (sec)	Range to Target (ft)	ξ (ft)	$\Delta\xi$ (ft)	ζ (ft)	$\Delta\zeta$ (ft)	Radial Difference (ft)
200	30	0	2.69	8.24	9702	8314.5	-1.2	-23.4	1.4	1.8
		30	3.60	9.56	10462	9198.6	1.0	-15.4	0.8	1.3
	60	0	4.82	3.68	6032	3373.9	0.2	-26.6	1.4	1.4
		30	5.05	4.58	6813	4628.4	1.8	-15.9	-0.7	1.9
	90	0	5.84	2.85	5025	500.4	0.4	-26.9	1.5	1.6
		30	5.84	3.58	5744	2828.7	1.8	-1.7	-0.3	1.8
300	30	0	3.87	8.46	10021	8684.5	-1.1	-35.9	1.0	1.5
		30	5.20	9.74	10728	9491.1	2.6	-23.6	0.9	2.8
	60	0	7.04	3.76	6193	3654.3	0.1	-41.5	0.6	0.6
		30	7.39	4.66	6961	4843.3	0.8	-26.0	0.2	0.8
	90	0	8.72	2.89	5056	749.2	0.3	-42.5	0.2	0.4
		30	8.72	3.62	5769	2877.7	0.2	-6.6	-0.5	0.5
400	30	0	4.97	8.67	10336	9046.1	-1.1	-49.0	-0.2	1.1
		30	6.69	9.91	10991	9787.4	2.3	-32.1	0.8	2.4
	60	0	9.13	3.84	6362	3933.2	-0.1	-57.5	-1.4	1.4
		30	9.62	4.74	7116	5063.6	-1.0	-37.5	-1.0	1.4
	90	0	11.56	2.94	5099	997.5	0.2	-60.0	-3.0	3.0
		30	11.56	3.67	5805	2949.5	-3.6	-14.6	-1.5	3.9

Table III

Comparison Between the Simplified Approximate Theory and the Old Approximate
Theory for a Gun Altitude of 8000 ft

V_A (knots)	E (deg)	A (deg)	Initial Yaw (deg)	Time of Flight (sec)	Range to Target (ft)	ξ (ft)	$\Delta\xi$ (ft)	ζ (ft)	$\Delta\zeta$ (ft)	Radial Difference (ft)
200	60	0	4.82	7.63	9510	5141.1	-0.8	-40.8	1.9	2.1
		30	5.05	9.23	10567	6904.1	1.0	-23.7	1.1	1.5
	90	0	5.84	5.96	8038	777.1	0.6	-42.0	2.1	2.2
		30	5.84	7.36	9095	4325.7	1.9	-2.5	-0.4	1.9
300	60	0	7.04	7.80	9740	5555.4	-0.7	-63.3	0.7	1.0
		30	7.39	9.40	10767	7206.4	0.5	-38.5	0.5	0.7
	90	0	8.72	6.03	8084	1162.6	0.3	-66.1	0.1	0.3
		30	8.72	7.41	9129	4397.9	-0.3	-9.9	-0.6	0.7
400	60	0	9.13	7.99	9979	5964.3	0.2	-87.4	-2.3	2.3
		30	9.62	9.57	10975	7513.6	-0.6	-55.4	-1.3	1.4
	90	0	11.56	6.12	8149	1546.5	0.1	-93.0	-4.6	4.6
		30	11.56	7.50	9180	4503.4	-5.5	-22.1	-2.1	5.9

and a depression angle of 107.9 deg. In these situations the initial yaw is 17.9 deg. The results of these computations are given in Table IV. The biggest component of the radial difference is seen to be $\Delta\zeta$. The amount of this difference for all three altitudes is about 3 mr, and this can be corrected in the simplified theory by adjusting the swerve parameters.

In all instances, the aircraft is assumed to be flying straight and level. The firing geometry is that of Fig. 15.

The complete new set of differential equations for trajectory computation is listed here for convenience as follows:

$$m \frac{du}{dP} = -\rho d^2 V K_{D_o} \left(V/V_{sd} \right) \left[1 + k_o e^{-kP} \right]$$

$$\frac{dt}{dP} = \frac{1}{u}$$

$$\frac{dD}{dP} = \frac{g}{u^2}$$

$$\frac{dQ}{dP} = D$$

where

$$V = u \sqrt{1 - 2D \sin \theta_o + D^2}$$

Definitions of symbols are in the List of Symbols at the front of this report. It is noted that these equations would be particle trajectory equations if the term

$$1 - k_o e^{-kP}$$

were deleted.

Integration of these equations yields gravity drop Q, time of flight t, and projectile velocity V versus pseudorange P. Projectile position in air mass coordinates is given by

$$\vec{R} = \vec{P} + \vec{Q} + \vec{S}$$

55

Table IV

Worst-Case Conditions for the Simplified Approximate Theory

V_A = 600 knots

A = 0 deg

E = 107.9 deg

Initial Yaw = 17.9 deg

Altitude (ft)	Time of Flight (sec)	Range to Target (ft)	ξ (ft)	$\Delta\xi$ (ft)	ζ (ft)	$\Delta\zeta$ (ft)	Radial Difference (ft)
2000	0.87	2000	4.7	-0.3	42.1	7.1	7.1
5000	3.24	5001	10.5	-1.7	103.0	17.0	17.1
8000	6.25	8002	16.0	-2.8	158.5	25.7	25.9

where $\vec{S}$ is the swerve. It is verified herein that $\vec{S}$ can be approximated adequately by the relation

$$S = \vec{C}P$$

where $\vec{C}$ is given in terms of initial conditions and two parameters a and b. Components of $\vec{R}$ in the air mass system are

$$\xi = P \cos \theta_o + C_\xi P$$

$$\eta = P \sin \theta_o + C_\eta P - Q$$

$$\zeta = C_\zeta P$$

where

$$C_\xi = -10^{-3} \delta_o \left(a \cos \phi_o - b \sin \phi_o \right) \sin \theta_o$$

$$C_\eta = 10^{-3} \delta_o \left(a \cos \phi_o - b \sin \phi_o \right) \cos \theta_o$$

$$C_\zeta = 10^{-3} \delta_o \left(a \sin \phi_o + b \cos \phi_o \right)$$

The ξ-axis lies along the horizontal projection of $\vec{P}$, η is vertical positive up, and ζ completes a right-handed coordinate system. Angles θ_o, δ_o, and ϕ_o are respectively the elevation angle of $\vec{P}$ above the horizontal, the initial yaw angle, and the initial precession angle.

The swerve approximation is based upon the observation that windage jump parameters X and Y (Refs. 1, 2, and 11) calculated by use of the Eglin code R370 are approximately constant after the projectile has traveled about 1000 ft, and are related to the yaw by approximately $X = a\delta_o$ and $Y = b\delta_o$.

Values of k and k_o in the differential equation for u can be obtained in several different ways as is discussed in the main body of this report. The method used for the calculations recorded in this section is borrowed from the old theory of Sterne (Refs. 5 and 6). The equations are as follows:

$$s_o = \frac{A^2 N^2}{4B\rho d^2 V_o^2 K_M}$$

$$k_o = \frac{s_o - 1/2}{s_o - 1} K_{D_\delta 2} \delta_o^2$$

$$c' = \frac{\rho_o d^2}{2m}\left[K_L + \frac{md^2}{B} K_H\right]$$

$$c'' = \frac{\rho_o d^2}{2m} K_{D_o}$$

$$c = c' + \frac{c''}{s_o - 1}$$

$$k = 2_\sigma c$$

Trajectory initial conditions are calculated from the following relations which are derived in Section II.

$$V_{ox} = V_A + V_m \cos A \cos E$$

$$V_{oy} = V_m \sin A$$

$$V_{oz} = -V_m \cos A \sin E$$

$$V_o = \sqrt{V_A^2 + 2V_A V_m \cos A \cos E + V_m^2}$$

$$\delta_o = \arccos \frac{V_m + V_A \cos A \cos E}{V_o}$$

$$V_{xy} = \sqrt{V_{ox}^2 + V_{oy}^2}$$

$$\sin \theta_o = \frac{V_{oz}}{V_o}$$

$$\cos \theta_o = \frac{V_{xy}}{V_o}$$

$$\sin B = \frac{V_{oy}}{V_{xy}}$$

$$\cos B = \frac{V_{ox}}{V_{xy}}$$

$$\cos \phi_o = - \frac{(\cos A \cos E \cos B + \sin A \sin B) \sin \theta_o + \cos A \sin E \cos \theta_o}{\sin \delta_o}$$

$$\sin \phi_o = \frac{\cos A \cos E \sin B - \sin A \cos B}{\sin \delta_o}$$

In addition $u = V_o$, $t = 0$, $D = 0$, and $Q = 0$ when $P = 0$.

The relation between ξ, η, ζ coordinates and x, y, z coordinates is

$$x = \xi \cos B + \zeta \sin B$$

$$y = \xi \sin B - \zeta \cos B$$

$$z = \eta$$

The x, y, z system is right handed, with x along the flight path and z vertical.

2. Modified Siacci Method

The modified Siacci method is applicable to both air-to-air and air-to-ground airborne fire-control computation. The basic difference between the two modes of operation is the kinematic lead prediction requirement for a moving target, occurring chiefly in the air-to-air encounter. Accurate kinematic prediction requires an accurate estimate of projectile time of flight as well as an almost instantaneous solution to the fire-control problem. The Siacci solutions provide a decided advantage in computation time over numerical integration of even the simplest forms of the equations of motion. It does not, however, yield equivalent accuracy in the time-of-flight calculation. For the 20-mm, M56 round, the Siacci

error in time of flight is less than 0.01 sec for trajectory ranges up
to 3,000 ft, but increases to values greater than 0.05 sec for ranges
beyond 5,000 ft. The time of flight is influenced by variations in air
density, thus increasing the error resulting from the Siacci method for
relatively high altitude, air-to-ground fire due to failure to account for
variations from the firing altitude air density. This effect is not of
consequence when altitude variations are not excessive (air-to-air), and
the time of flight is not usually needed to a high degree of accuracy for
air-to-ground fire control. Corrections for the air-density variation
have been derived (Ref. 2) but will not be considered here.

For the purpose of comparison, air-to-ground trajectories for a
turreted gun were computed by the modified Siacci method and the ap-
proximate equations of motion. Air-to-ground trajectories were selected
over air-to-air because of the larger projectile yaw angles which are a
major shortcoming of the basic Siacci theory. The intention is to dem-
onstrate that the modified Siacci equations are capable of accurate large-
yaw ballistic calculations for moderate ranges. Calculations were made
for a set of initial conditions similar to those used for the modified point-
mass equations computations, and the results are to be found in Tables V,
VI, and VII. As before, altitudes of 2000 ft, 5000 ft, and 8000 ft, and
aircraft speeds of 200 knots, 300 knots, and 400 knots are used. Gun
depression angles are 30 deg, 60 deg, and 90 deg and traverse angles
are 0 deg and 30 deg. The gun-pointing error is seen to be less than
1 mr for all ranges below 5000 ft, no greater than 2 mr for ranges up
to 8000 ft, and as high as 5.1 mr for ranges slightly above 9000 ft. The
largest errors occur at the higher altitudes and longer ranges due, in
part, to the variation in air density and the breakdown of the approxima-
tion V = u (Section II). However, the modified Siacci method yields a
highly accurate representation of the approximate-equation solution for
yaw angles as high as 11.56 deg and some ranges greater than 8000 ft.
The results of worst-case calculations are shown in Table VIII. The
results are about the same as those for the worst-case, modified point-
mass calculations of Table IV, and the reason is the same; the windage
jump approximation can be improved for these conditions.

As a last, but important, word on comparison of the modified
Siacci method with more accurate forms of ballistic equations, three
FORTRAN ballistics computer codes were compared for relative speed
of computation. The modified Siacci code was compared with modified
point-mass integration and the approximate equations of motion. Though
no attempt was made to optimize the coding of the three programs, it
is believed that ratios of the computation times should be fairly repre-
sentative of what would be experienced in an airborne fire-control com-
putation . The relative times vary from one trajectory to another as
functions of range and step size of the numerical integration; but, for
the trajectories considered, the Siacci method appears to be 20 to 100
times as fast as the modified point-mass integration, and 500 to 1500
times as fast as numerical integration of the approximate equations of

Table V

Comparison Between the Modified Siacci Method and the Old Approximate Calculations for a Gun Altitude of 2,000 ft

V_A (knots)	E (deg)	A (deg)	Initial Yaw (deg)	Range to Target (ft)	ξ (ft)	$\Delta\xi$ (ft)	ζ (ft)	$\Delta\zeta$ (ft)	Radial Difference (ft)	Gun Pointing Difference (mr)
200	30	0	2.69	4275	3778.2	-1.6	-10.6	0.7	1.7	0.2
		30	3.60	4802	4366.3	-2.0	-7.3	0.4	2.0	0.2
	60	0	4.82	2431	1381.8	0.1	-10.9	0.6	0.6	0.3
		30	5.05	2774	1922.0	0.7	-6.6	0.3	0.8	0.2
	90	0	5.84	2010	203.0	0.2	-10.9	0.6	0.6	0.3
		30	5.84	2311	1157.2	0.8	-0.6	0.0	0.8	0.3
300	30	0	3.87	4449	3973.6	-2.1	-16.4	0.5	2.2	0.2
		30	5.20	4961	4540.2	-2.8	-11.3	0.4	2.8	0.2
	60	0	7.04	2499	1498.0	0.0	-17.0	0.2	0.2	0.1
		30	7.39	2838	2013.7	0.2	-10.8	0.1	0.2	0.1
	90	0	8.72	2023	304.0	0.1	-17.2	0.1	0.1	0.1
		30	8.72	2321	1177.8	0.1	-2.6	-0.1	0.1	0.1
400	30	0	4.97	4623	4168.1	-3.0	-22.5	0.0	3.0	0.3
		30	6.69	5120	4713.6	-4.9	-15.6	0.2	4.9	0.4
	60	0	9.13	2570	1614.0	-0.2	-23.6	-0.6	0.6	0.2
		30	9.62	2906	2108.2	-1.1	-15.6	-0.4	1.2	0.3
	90	0	11.56	2041	404.9	0.0	-24.4	-1.3	1.3	0.6
		30	11.56	2336	1207.9	-1.6	-5.9	-0.5	1.7	0.6

Table VI

Comparison Between the Modified Siacci Method and the Old Approximate Calculations
for a Gun Altitude of 5,000 ft

V_A (knots)	E (deg)	A (deg)	Initial Yaw (deg)	Range to Target (ft)	ξ (ft)	$\Delta\xi$ (ft)	ζ (ft)	$\Delta\zeta$ (ft)	Radial Difference (ft)	Gun Pointing Difference (mr)
200	60	0	4.82	6032	3373.9	-6.9	-26.6	1.5	7.1	1.0
		30	5.05	6813	4628.4	-14.0	-15.9	0.8	14.0	1.5
	90	0	5.84	5025	500.4	-0.1	-26.9	1.5	1.5	0.3
		30	5.84	5744	2828.7	-3.6	-1.7	-0.3	3.6	0.5
300	60	0	7.04	6193	3654.3	-8.0	-41.5	0.7	8.0	1.0
		30	7.39	6961	4843.3	-16.4	-26.0	0.3	16.4	1.7
	90	0	8.72	5056	749.2	-0.5	-42.5	0.2	0.5	0.1
		30	8.72	5769	2877.7	-5.5	-6.6	-0.5	5.5	0.8
400	60	0	9.13	6362	3933.2	-9.3	-57.5	-1.3	9.4	1.2
		30	9.62	7116	5063.6	-20.1	-37.5	-0.9	20.1	2.0
	90	0	11.56	5099	997.5	-0.9	-60.0	-2.9	3.0	0.6
		30	11.56	5805	2949.5	-9.6	-14.6	-1.4	9.7	1.4

Table VII

Comparison Between the Modified Siacci Method and the Old Approximate Calculations
for a Gun Altitude of 8,000 ft

V_A (knots)	E (deg)	A (deg)	Initial Yaw (deg)	Range to Target (ft)	ξ (ft)	$\Delta\xi$ (ft)	ζ (ft)	$\Delta\zeta$ (ft)	Radial Difference (ft)	Gun Pointing Difference (mr)
200	90	0	5.84	8038	777.1	-4.1	-42.0	2.4	4.8	0.6
		30	5.84	9095	4325.7	-42.3	-2.5	-0.3	42.3	4.1
300	90	0	8.72	8084	1162.6	-6.8	-66.1	0.5	6.8	0.8
		30	8.72	9129	4397.9	-46.2	-9.9	-0.5	46.2	4.4
400	90	0	11.56	8149	1546.5	-9.7	-93.0	-4.1	10.5	1.3
		30	11.56	9180	4503.4	-54.1	-22.1	-1.8	54.1	5.1

Table VIII

Worst-Case Conditions for the Modified Siacci Method

V_A = 600 knots   A = 0 deg   E = 107.9 deg

Initial Yaw = 17.9 deg

Altitude (ft)	Range to Target (ft)	ξ (ft)	$\Delta\xi$ (ft)	ζ (ft)	$\Delta\zeta$ (ft)	Radial Difference (ft)	Gun-Pointing Difference (mr)
2000	2000	4.7	-0.3	42.1	7.1	7.1	3.6
5000	5001	10.5	-1.7	103.0	16.9	17.0	3.4
8000	8002	16.0	-2.9	158.5	24.7	24.9	3.1

motion. Representative calculation times obtained by use of the CDC 3200 computer are 0.01 sec for the Siacci method, 0.5 sec for point-mass integration, and 10 sec for the approximate equations of motion.

If the modified Siacci approach is to be used in airborne calculations, the same equation set as that listed above for the modified point-mass equations may be used, except the set of differential equations is deleted and replaced with the Siacci equations as follows:

$$S(u/a_o) = S(u_o/a_o) + \frac{\sigma}{C} P + \frac{k_o}{2cC}$$

$$Q = \left(\frac{C}{\sigma a_o}\right)^2 \left[A(u/a_o) - A(u_o/a_o) - I(u_o/a_o) \frac{\sigma}{C} P\right]$$

$$t = \frac{C}{\sigma a_o} \left[T(u/a_o) - T(u_o/a_o)\right]$$

The functions S, T, A, and I are precomputed at a ground-based facility and are made available onboard in tabular form (Refs. 2 and 9) or as curve fits (Appendix I).

3. Polynomial Curve Fitting of Ballistic Lead Angles

Polynomial curve fitting of ballistic leads by exact fit to the data points appears to have promise in some instances for turreted gun systems that have large fields-of-coverage and require fast computation speed. The reduction of the amount of data that must be stored if curve fitting is used in place of tables, and the computation time reduction if it is used in place of numerical integration, are obvious advantages. The curve fits of ballistic leads obtained in this study by means of the Siacci method indicate the ease of accurate curve fitting. The curve-fit coefficients are listed in Tables XVIII, XIX, and XX of Appendix IV. Extension of the method to the curve fitting of ballistic leads obtained by more exact and complex forms of trajectory computation should present no problem.

The accuracy of the curve fits obtained in this study was tested by computation of the lead angles at all points midway between all data points of the grid used to generate the coefficient. Comparison of the leads derived from Siacci calculations with the curve fit gives an indication of the curve-fit accuracy obtained. The complete results of this comparison are listed in Tables XIV, XV, and XXI of Appendix II. A summary of the error analysis is given in Table IX below.

65

Table IX

Accuracy of Curve Fits as Compared with Siacci Calculations

Lead Angle	Depression Angle Interval	Maximum Error (mr)	Average Error (mr)
ΔE	$30^\circ \leq E_T \leq 90^\circ$	1.50	0.61
	$90^\circ \leq E_T \leq 135^\circ$	1.28	0.41
ΔA	$30^\circ \leq E_T \leq 135^\circ$	0.89	0.35

$$0.86 \leq \sigma \leq 0.98 \qquad 200 \text{ ft/sec} \leq V_A \leq 800 \text{ ft/sec}$$

$$130^\circ \leq A_T \leq 30^\circ$$

The accuracy could be increased or relaxed to any desired level which would show a corresponding increase or reduction of the number of coefficients required for the curve fit. With the accuracy obtained in this example, 360 coefficients are required for ΔE and 144 coefficients are required for ΔA. Thus, a total of 504 coefficients would have to be stored in the onboard computer of the fire-control system. In the case of tabular trajectory-table storage, many times this amount of data would need to be stored to obtain equivalent accuracy.

4. Sensitivity of Ballistics Calculations

In Section III, a comparison was made between the results of calculations performed using the Siacci method and computations made by use of the approximate equations of Ref. 1. A similar comparison was made in this section, and the results of Section III were poor relative to these. The reason for this discrepancy is thought to be due to the fact that this laboratory did not use the same numerical values for certain ballistic parameters (such as the projectile mass) as did Eglin, since the approximate calculations of Section III were performed at Eglin Air Force Base, whereas those of this section were done at this laboratory. This indicates that the results of ballistics calculations are sensitive to small errors in ballistics parameters, and one might expect differences of the order of one degree between calculations made by different laboratories. Note should be taken of the implications of this statement with regard to fire-control system design.

APPENDIX I

CURVE-FIT COEFFICIENTS FOR THE SIACCI FUNCTIONS

The Siacci functions (S, T, I, and A) were curve fitted as fourth-degree polynomials over segments of the data listed in Ref. 10. The tabulated values of S were curve fitted as a function of U, while the values of T, I, and A were fitted as functions of S as indicated below.

$$S = a_0 + a_1 X + a_2 X^2 + a_3 X^3 + a_4 X^4$$

$$[T, I, \text{ or } A] = b_0 + b_1 Y + b_2 Y^2 + b_3 Y^3 + b_4 Y^4$$

The functional forms of the independent variables X and Y are given by

$$X = 4\left(\frac{U_{max} - U}{U_{max} - U_{min}}\right)$$

and

$$Y = 4\left(\frac{S - S_{max}}{S_{max} - S_{min}}\right)$$

The terms U_{max}, U_{min}, S_{max}, and S_{min} represent the upper and lower bounds of the curve fit intervals as shown in the tables. The values of a_i and b_i are also given in Tables X through XIII for specified intervals of U and S.

Table X

Coefficients for S vs U

$U_{max} - U_{min}$ (ft/sec)	a_0	a_1	a_2	a_3	a_4
7,000 - 5,000	0	1.36847×10^3	2.54383×10^1	6.38333×10^{-1}	6.16667×10^{-2}
5,000 - 3,000	5.93754×10^3	1.61767×10^3	4.08571×10^1	7.75833×10^{-1}	3.62917×10^{-1}
3,000 - 1,400	1.32045×10^4	1.68706×10^3	1.29875×10^1	1.24033×10^1	9.25000×10^{-2}
1,400 - 1,200	2.09780×10^4	3.02091×10^2	4.89875×10^0	3.89167×10^{-1}	2.12500×10^{-2}
1,200 - 1,000	2.22951×10^4	4.52635×10^2	-1.46066×10^2	8.01750×10^1	-8.90417×10^0

68

Table XI

Coefficients for T vs S

$S_{min} - S_{max}$	b_0	b_1	b_2	b_3	b_4
0 - 5937.54	0	2.12021×10^{-1}	8.28375×10^{-3}	2.74167×10^{-4}	2.12500×10^{-5}
5,937.54 - 9,348.33	1.00361×10^{0}	1.70512×10^{-1}	4.52917×10^{-3}	1.03333×10^{-4}	5.83333×10^{-6}
9,348.33 - 13,204.51	1.76623×10^{0}	2.41006×10^{-1}	8.06792×10^{-3}	2.64167×10^{-4}	1.20833×10^{-5}
13,204.51 - 20,978.03	2.87934×10^{0}	6.46825×10^{-1}	5.20925×10^{-2}	3.20000×10^{-3}	6.52500×10^{-4}
20,978.03 - 22,295.12	6.67196×10^{0}	2.35188×10^{-1}	4.65625×10^{-3}	2.25000×10^{-5}	3.75000×10^{-6}
22.295.12 - 24,620.34	7.68961×10^{0}	4.81979×10^{-1}	2.09521×10^{-2}	-2.51917×10^{-3}	2.07917×10^{-4}

Table XII

Coefficients for I vs S

$S_{min} - S_{max}$	b_0	b_1	b_2	b_3	b_4
0 - 5,937.54	0	9.64167×10^{-4}	9.10833×10^{-5}	-2.66667×10^{-6}	1.41667×10^{-6}
5,937.54 - 13,204.51	5.50600×10^{-3}	2.36325×10^{-3}	2.24375×10^{-4}	3.62500×10^{-5}	2.12500×10^{-6}
13,204.51 - 20,978.03	2.14130×10^{-2}	6.81075×10^{-3}	1.33696×10^{-3}	-1.67500×10^{-5}	5.80417×10^{-5}
20,978.03 - 22,295.12	8.38340×10^{-2}	4.81392×10^{-3}	1.24404×10^{-3}	-5.11917×10^{-4}	7.39583×10^{-5}
22,295.12 - 24,620.34	1.09165×10^{-1}	1.28353×10^{-2}	1.14596×10^{-3}	-1.24750×10^{-4}	1.05417×10^{-5}

70

Table XIII

Coefficients for A vs S

$S_{min} - S_{max}$	b_0	b_1	b_2	b_3	b_4
0 - 5937.54	0	-1.00000×10^{-3}	7.36667×10^{-1}	3.00000×10^{-2}	3.33333×10^{-3}
5,937.54 - 13,204.51	1.45200×10^{1}	9.96250×10^{0}	2.21042×10^{0}	1.02500×10^{-1}	2.45833×10^{-2}
13,204.51 - 16,731.28	1.02590×10^{2}	1.88817×10^{1}	1.39500×10^{0}	5.83333×10^{-2}	5.00000×10^{-3}
16,731.28 - 20,978.03	2.05450×10^{2}	4.10850×10^{1}	3.77750×10^{0}	2.20000×10^{-1}	2.75000×10^{-2}
20,978.03 - 22,295.12	4.51350×10^{2}	2.76133×10^{1}	8.80000×10^{-1}	2.66667×10^{-2}	1.55220×10^{-9}
22,295.12 - 24,620.34	5.77590×10^{2}	6.34100×10^{1}	3.83333×10^{0}	1.60000×10^{-1}	-3.33333×10^{-3}

APPENDIX II

ACCURACY OF THE BALLISTIC LEAD POLYNOMIAL CURVE FITS

The following tables are the results of a comparison of the polynomial curve fits of the depression and deflection ballistic lead angles with the values derived by Siacci calculations. The comparison is made at the mid-point between all data points of the grid used to generate the coefficients. The average error should, in reality, be less than the average error shown here because the curve fit is, in general, more accurate near the data points. The error columns in the tables are the Siacci values minus the curve-fit values in milliradians.

Table XIV

Depression Lead Angle Comparison

$Y_T = 0.0 \text{ ft}$ $\qquad -30^\circ \le A_T \le 30^\circ$

$0.86 \le \sigma \le 0.98$

$200 \text{ ft/sec} \le V_A \le 800 \text{ ft/sec}$ $\qquad 30^\circ \le E_T \le 90^\circ$

Y_A (ft)	σ	V_A (ft/sec)	A_T (deg)	E_T (deg)	Curve Fit (deg)	ΔE Siacci (deg)	Error (mr)
3929	.89	350	-20	37.50	-2.294	-2.362	-1.1854
3929	.89	350	-20	52.50	-4.500	-4.511	-0.1817
3929	.89	350	-20	67.50	-5.710	-5.713	-0.0662
3929	.89	350	-20	82.50	-6.393	-6.351	.7364
3929	.89	350	0	37.50	-2.369	-2.405	-0.6322
3929	.89	350	0	52.50	-4.255	-4.269	-0.2323
3929	.89	350	0	67.50	-5.325	-5.353	-0.4829
3929	.89	350	0	82.50	-5.949	-5.949	-0.0059
3929	.89	350	20	37.50	-2.268	-2.339	-1.2259
3929	.89	350	20	52.50	-4.471	-4.481	-0.1657
3929	.89	350	20	67.50	-5.667	-5.678	-0.1922
3929	.89	350	20	82.50	-6.357	-6.330	.4730
3929	.89	650	-20	37.50	-5.904	-5.968	-1.1115
3929	.89	650	-20	52.50	-9.108	-9.092	.2714
3929	.89	650	-20	67.50	-11.019	-10.986	.5747
3929	.89	650	-20	82.50	-12.028	-11.942	1.4968
3929	.89	650	0	37.50	-5.610	-5.673	-1.1060
3929	.89	650	0	52.50	-8.414	-8.440	-0.4487
3929	.89	650	0	67.50	-10.163	-10.199	-0.6303
3929	.89	650	0	82.50	-11.158	-11.160	-0.0355
3929	.89	650	20	37.50	-5.812	-5.885	-1.2671
3929	.89	650	20	52.50	-9.007	-8.989	.3248
3929	.84	650	20	67.50	-10.874	-10.868	.1181
3929	.89	650	20	82.50	-11.912	-11.879	.5687
1743	.95	350	-20	37.50	-3.704	-3.662	.7608
1743	.95	350	-20	52.50	-5.065	-5.017	.8409
1743	.95	350	-20	67.50	-5.967	-5.938	.5099
1743	.95	350	-20	82.50	-6.449	-6.414	.6120
1743	.95	350	0	37.50	-3.455	-3.423	.5682
1743	.95	350	0	52.50	-4.686	-4.674	.1971
1743	.95	350	0	67.50	-5.531	-5.540	-0.1627
1743	.95	350	0	82.50	-5.999	-6.007	-0.1424
1743	.95	350	20	37.50	-3.679	-3.639	.7082
1743	.95	350	20	52.50	-5.036	-4.987	.8573
1743	.95	350	20	67.50	-5.924	-5.903	.3770
1743	.95	350	-20	82.50	-6.413	-6.393	.3491
1743	.95	650	-20	37.50	-7.283	-7.199	1.4576
1743	.95	650	-20	52.50	-0.654	-9.581	1.2861
1743	.95	650	-20	67.50	-11.210	-11.210	1.1263
1743	.95	650	-20	42.50	-12.078	-12.003	1.2970
1743	.95	650	0	37.50	-2.647	-2.617	.5136
1743	.95	650	0	52.50	-8.831	-8.832	-0.0173
1743	.95	650	0	67.50	-10.375	-10.391	-0.2755
1743	.95	650	0	82.50	-11.212	-11.222	-0.1679
1743	.95	650	20	37.50	-7.191	-7.116	1.3032
1743	.95	650	20	52.50	-9.554	-9.477	1.3382
1743	.95	650	20	67.50	-11.129	-11.091	.6610
1743	.95	650	20	82.50	-11.961	-11.940	.3686

Table XV

Depression Lead Angle Comparison

$0.86 \le \sigma \le 0.98$ $Y_T = 0.0 \text{ ft}$ $-30^\circ \le A_T \le 30^\circ$

$200 \text{ ft/sec} \le V_A \le 800 \text{ ft/sec}$ $90^\circ \le E_T \le 135^\circ$

Y_A (ft)	σ	V_A (ft/sec)	A_T (deg)	E_T (deg)	ΔE Curve Fit (deg)	ΔE Siacci (deg)	Error (mr)
3929	.87	350	-20	95.63	-6.524	-6.511	.2393
3929	.87	350	-20	106.88	-6.440	-6.414	.4615
3929	.87	350	-20	118.13	-6.197	-6.160	.6424
3929	.87	350	-20	129.38	-5.901	-5.860	.7079
3929	.87	350	0	95.63	-5.105	-6.120	-0.2545
3929	.87	350	0	106.88	-6.022	-6.032	-0.1826
3929	.87	350	0	118.13	-5.767	-5.776	-0.1549
3929	.87	350	0	129.38	-5.640	-5.449	-0.1619
3929	.87	350	20	95.63	-6.564	-6.533	.5423
3929	.87	350	20	106.88	-6.488	-6.451	.6513
3929	.87	350	20	118.13	-6.232	-6.191	.6629
3929	.87	350	20	129.38	-5.931	-5.887	.7560
3929	.87	650	-20	95.63	-12.051	-12.038	.2292
3929	.87	650	-20	106.88	-11.723	-11.693	.5242
3929	.87	650	-20	118.13	-11.076	-11.030	.7917
3929	.87	650	-20	129.38	-10.197	-10.163	.5998
3929	.87	650	0	95.63	-11.350	-11.363	-0.2305
3929	.87	650	0	106.88	-11.078	-11.089	-0.1964
3929	.87	650	0	118.13	-10.452	-10.465	-0.2300
3929	.87	650	0	129.38	-9.587	-9.609	-0.3797
3929	.87	650	20	95.63	-12.196	-12.123	1.2765
3929	.87	650	20	106.88	-11.589	-11.823	1.1532
3929	.87	650	20	118.13	-11.191	-11.144	.8279
3929	.87	650	20	129.38	-10.296	-10.253	.7323
1743	.95	350	-20	95.63	-6.456	-6.449	.1695
1743	.95	350	-20	106.88	-6.230	-6.227	.0661
1743	.95	350	-20	118.13	-5.789	-5.790	-0.0216
1743	.95	350	-20	129.38	-5.157	-5.167	-0.1826
1743	.95	350	0	95.63	-6.060	-6.075	-0.2561
1743	.95	350	0	106.88	-5.864	-5.884	-0.3137
1743	.95	350	0	118.13	-5.455	-5.679	-0.4181
1743	.95	350	0	129.38	-4.890	-4.890	-0.5524
1743	.95	350	20	95.63	-6.495	-6.471	.4127
1743	.95	350	20	106.88	-6.278	-6.263	.2561
1743	.95	350	20	118.13	-5.824	-5.824	-0.0013
1743	.95	350	20	129.38	-5.187	-5.195	-0.1349
1743	.95	650	-20	95.63	-11.967	-11.964	.0478
1743	.95	650	-20	106.88	-11.482	-11.476	.1061
1743	.95	650	-20	118.13	-10.615	-10.603	.2164
1743	.95	650	-20	129.38	-9.392	-9.375	.1173
1743	.95	650	0	95.63	-11.301	-11.314	-0.2235
1743	.95	650	0	106.88	-10.901	-10.922	-0.3183
1743	.95	650	0	118.13	-10.498	-10.123	-0.4248
1743	.95	650	0	129.38	-8.939	-8.966	-0.4664
1743	.95	650	20	95.63	-12.111	-12.049	1.0953
1743	.95	650	20	106.88	-11.644	-11.606	.7362
1743	.95	650	20	118.13	-10.731	-10.717	.2534
1743	.95	650	20	129.38	-9.479	-9.465	.2501

Table XVI

Deflection Lead Angle Comparison

$0.86 \leq \sigma \leq 0.98$ $y_T = 0.0$ ft $-30° \leq A_T \leq 30°$

200 ft/sec $\leq V_A \leq 800$ ft/sec $30° \leq E_T \leq 135°$

γ_A (deg)	σ	V_A (ft/sec)	A_T (deg)	E_T (deg)	ΔE Curve Fit (deg)	ΔE Siacci (deg)	Error (mr)
3929	.89	350	-20	47.50	1.690	1.653	-0.6375
3929	.89	350	-20	82.50	.373	.361	-0.2164
3929	.89	350	-20	117.50	-0.782	-0.795	-0.2197
3929	.89	350	0	47.50	-0.010	-0.013	-0.0522
3929	.89	350	0	82.50	-0.019	-0.004	.2613
3929	.89	350	0	117.50	-0.020	-0.012	.1348
3929	.89	350	20	47.50	-1.722	-1.690	.5623
3929	.89	350	20	82.50	-0.432	-0.442	-0.1897
3929	.89	350	20	117.50	.729	.751	.3761
3929	.89	650	-20	47.50	2.695	2.654	-0.7186
3929	.89	650	-20	82.50	-1.887	-1.873	-0.7779
3929	.89	650	-20	117.50	.268	.223	.2542
3929	.89	650	0	47.50	-0.040	-0.048	-0.1503
3929	.89	650	0	82.50	-0.066	-0.016	.8892
3929	.89	650	0	117.50	-0.062	-0.039	.4052
3929	.89	650	20	47.50	-2.821	-2.789	.5597
3929	.89	650	20	82.50	-0.469	-0.508	-0.6895
3929	.89	650	20	117.50	1.721	1.731	.1711
1743	.95	350	-20	47.50	1.402	1.401	-0.0192
1743	.95	350	-20	82.50	.191	.188	-0.0534
1743	.95	350	-20	117.50	-1.013	-0.999	.2418
1743	.95	350	0	47.50	-0.011	-0.013	-0.0505
1743	.95	350	0	82.50	-0.019	-0.004	-0.2600
1743	.95	350	0	117.50	-0.020	-0.012	.1369
1743	.95	350	20	47.50	-1.435	-1.438	-0.0516
1743	.95	350	20	82.50	-0.249	-0.270	-0.3543
1743	.95	350	20	117.50	.960	.955	-0.0821
1743	.95	650	-20	47.50	2.394	2.398	.0762
1743	.95	650	-20	82.50	.075	.039	-0.6170
1743	.95	650	-20	117.50	-2.128	-2.092	.6279
1743	.95	650	0	47.50	-0.040	-0.049	-0.1449
1743	.95	650	0	82.50	-0.066	-0.015	.8845
1743	.95	650	0	117.50	-0.067	-0.038	.4133
1743	.95	650	20	47.50	-2.522	-2.535	-0.2203
1743	.95	650	20	82.50	-0.274	-0.323	-0.8557
1743	.95	650	20	117.50	1.962	1.951	-0.1897

75

APPENDIX III

COMPARISON OF THE SIACCI CALCULATIONS WITH THE EGLIN 20-mm FIRING TABLES

Selected values of the independent variables were used to compare the curve fit of the Siacci calculations and the Eglin firing tables for the M56, 20-mm round. From the table, an evaluation of the accuracy of the Siacci calculations was made.

Table XVII

Comparison of Lead Angles Derived from the Firing Tables and Siacci Calculations

Y_A	V_A	A_T	E_T	Siacci		Firing Tables	
				ΔE	ΔA	ΔE	ΔA
(ft)	(ft/sec)	(deg)	(deg)	(deg)	(deg)	(deg)	(deg)
2000	300	4.74	39.76	-5.37	-0.58	-5.25	-0.26
2000	300	5.00	57.83	-7.33	-0.42	-7.17	-0.00
2000	300	5.17	76.77	-8.54	-0.18	-8.23	-0.17
2000	300	3.60	96.66	-8.83	0.03	-10.34	-1.40
2000	300	22.52	39.55	-5.82	-2.64	-5.45	-2.48
2000	300	23.26	57.44	-8.03	-1.81	-7.56	-1.74
2000	300	23.99	76.02	-9.35	-0.75	-8.98	-10.08
2000	300	24.37	95.02	-9.71	0.45	-9.98	-0.63
5000	300	46.60	41.07	-4.07	-0.68	-3.93	-0.34
5000	300	49.28	58.34	-6.84	-0.49	-6.66	-0.07
5000	300	51.04	76.95	-8.37	-0.25	-8.05	-0.10
5000	300	35.34	94.62	-8.89	-0.02	-10.38	-1.47
5000	300	22.01	41.30	-4.07	-3.15	-3.70	-2.99
5000	300	22.87	58.15	-7.32	-2.23	-6.85	-2.14
5000	300	23.62	76.28	-9.10	-1.12	-8.72	-1.38
5000	300	23.96	94.92	-9.82	0.03	-10.08	-1.04
2000	450	4.64	37.53	-7.77	-0.87	-7.47	-0.36
2000	450	4.98	54.70	-10.67	-0.66	-10.30	-0.02
2000	450	5.29	72.90	-12.62	-0.34	-12.01	0.29
2000	450	8.40	93.28	-13.47	0.20	-11.72	3.40
2000	450	21.44	37.23	-8.44	-3.81	-7.77	-3.56
2000	450	22.41	54.17	-11.67	-2.74	-10.83	-2.59
2000	450	23.41	71.95	-13.77	-1.27	-13.05	-1.59
2000	450	25.56	90.43	-14.77	0.49	-14.57	0.56
5000	450	4.56	38.92	-6.39	-0.96	-6.08	-0.44
5000	450	4.92	55.28	-10.13	-0.74	-9.73	-0.08
5000	450	5.23	73.14	-12.38	-0.41	-11.86	0.23
5000	450	8.28	93.26	-13.52	0.07	-11.74	3.28
5000	450	20.98	39.06	-6.59	-4.29	-5.95	-4.03
5000	450	22.05	54.93	-10.88	-3.14	-10.07	-2.95
5000	450	23.03	72.32	-13.42	-1.64	-12.68	-1.97
5000	450	25.11	90.44	-14.79	0.02	-14.56	0.11

APPENDIX IV

BALLISTIC LEAD POLYNOMIAL CURVE-FIT COEFFICIENTS

The following tables contain the coefficients obtained from the direct polynomial curve fit of the ballistic lead angles derived from Siacci calculations for a turreted, air-to-ground, M61 gun. The target is assumed to be at sea level and the aircraft is flying straight and level. Effects due to aircraft attitude variation and wind velocity are not included. The four independent variables cover the following ranges:

$$200 \text{ ft/sec} \le V_A \le 800 \text{ ft/sec} \qquad -30 \text{ deg} \le A_T \le 30 \text{ deg}$$

$$0.86 \le \sigma \le 0.98 \qquad 30 \text{ deg} \le E_T \le 135 \text{ deg}$$

Tables XVIII and XIX list the depression leads for line-of-sight depression angles from 30 deg to 90 deg and 90 deg to 135 deg, respectively. Table XX contains the deflection leads for all values of the independent variables within the ranges specified above. The coefficients $A_{ijk\ell}$ are defined by the following polynomial.

$$\text{Lead Angle} = A_{1111} + A_{1112} \, w^0 x^0 y^0 z^1$$

$$+ A_{1122} \, w^0 x^0 y^1 z^1 + \ldots$$

$$+ A_{KLMN} \, w^{K-1} x^{L-1} y^{M-1} z^{N-1}$$

where w, x, y, and z are defined by Eq. (91) in Section III. The values of the subscripts (K, L, M, N) are equal to the number of data points for each independent variable used in the curve fit.

The coefficients are presented in standard FORTRAN "E" format. As an example, $5.01326E-04$ is equivalent to 5.01326×10^{-4}.

Table XVIII

Depression Lead Coefficients for Depression Angles Between 30 deg and 90 deg

ℓ

k	1	2	3	4	5	
1	-7.2970E 00	-1.2681F 00	2.8360E-01	-1.7781E-02	9.0373E-03	
2	4.2043E-02	3.0042E-02	1.1567E-02	-8.8609E-03	-5.1010E-03	$i = 1$
3	-5.6609E-01	-3.1685F-02	4.1921E-02	-1.4900F-02	4.7399F-03	
4	-6.5459E-03	-1.5111E-02	-7.1654E-03	3.5201E-03	2.2659E-03	
1	-2.9505E-01	1.4875E-01	-7.4276E-02	6.1103E-02	-1.8486E-02	
2	7.7645E-05	-4.3090F-05	8.6265E-06	-3.2416E-05	1.6828E-05	$i = 2$
3	-8.1352F-02	6.0855F-02	-3.2303E-02	1.3194F-02	-2.5402F-03	
4	-1.4067E-04	7.5965E-05	1.0582E-05	4.1452E-06	-3.1043E-06	
1	1.1407E-01	-9.5557F-02	4.9567E-02	-3.1909E-02	8.4272F-03	
2	-3.2371E-05	2.0328E-05	-7.8831E-06	1.7413E-05	-7.9922E-06	$i = 3$
3	4.4115E-02	-5.0744E-02	2.0836E-02	6.8630F-04	-2.3742F-03	
4	6.2701E-05	-4.0344E-05	-2.4860E-07	-7.3372E-07	5.4899E-07	

(a) $j = 1$

79

Table XVIII (continued)

		ℓ			
	1	**2**	**3**	**4**	**5**
1	-4.5327E 00	-6.9487E-01	1.4767E-01	1.3083E-02	-2.4990E-03
2	5.1910E-02	3.6395E-02	1.3816E-02	-1.1003E-02	-6.2565E-03
3	-4.1871E-01	-4.5511E-03	2.3859E-02	-2.5122E-03	1.6913E-04
4	-9.4147E-03	-1.9396E-02	-8.6224E-03	4.4775E-03	2.8073E-03
1	1.1750E-03	-1.8987E-02	1.1704E-02	5.2238E-04	-9.5374E-04
k 2	8.8681E-05	-4.4527E-05	-3.8147E-08	-3.3074E-05	2.1603E-05
3	6.7529E-03	2.2411E-03	-1.9402E-03	3.1252E-03	-1.1948E-03
4	-1.5817E-04	1.2337E-04	1.0526E-05	3.3903E-06	-4.9708E-06
1	-1.3749E-03	1.2582E-02	-6.5543E-03	-4.7295E-03	2.5573E-03
2	-3.6737E-05	1.9512E-05	-3.9166E-06	2.0124E-05	-1.0417E-05
3	-2.7037E-03	-1.8087E-03	2.4717E-03	-2.3719E-03	5.9147E-04
4	7.0656E-05	-6.3654E-05	3.2791E-06	-6.7597E-07	9.5796E-07

i = 2 (second block)
i = 3 (third block)

(b) j = 2

Table XVIII (concluded)

			ℓ		
	1	2	3	4	5
1	-1.5970E-02	-1.3622E-02	3.1076E-04	3.4909E-04	8.1994E-05
2	1.6427E-02	1.1141E-02	4.1125E-03	-3.5204E-03	-1.9573E-03
3	-2.8492E-02	1.5457E-02	4.1251E-03	-9.0144E-04	-1.0649E-04
4	-3.7644E-03	-6.5608E-03	-2.5935E-03	1.4933E-03	8.9395E-04
1	-5.9006E-03	2.8871E-03	6.4887E-05	-6.6485E-04	3.2086E-04
2	2.4833E-05	-9.8915E-06	-5.9687E-06	-6.3791E-06	7.2962E-06
3	-4.0964E-04	5.0262E-04	2.0597E-04	1.5803E-05	-4.4021E-05
4	-4.1105E-05	5.6163E-05	1.9120E-06	1.2830E-07	-2.2846E-06
1	2.4767E-03	-1.4394E-03	-3.2255E-04	9.9181E-04	-3.8889E-04
2	-1.0124E-05	3.4296E-06	1.9644E-06	5.3970E-06	-3.9824E-06
3	7.5524E-05	3.5053E-04	-5.6082E-04	-8.8412E-05	1.1566E-04
4	1.8415E-05	-2.8067E-05	3.0448E-06	-1.2226E-07	4.9780E-07

$i = 1$ (rows k=1–4, first block)

$i = 2$ (rows k=1–4, second block)

$i = 3$ (rows k=1–4, third block)

k

(c) $j = 3$

81

Table XIX

Depression Lead Coefficients for Depression Angles
Between 90 deg and 135 deg

	ℓ 1	2	3	4	5	
1	-8.2069E 00	5.4353E-01	1.3518E-01	-1.1245E-02	-2.0958E-03	
2	-5.0673E-02	2.9277E-02	-8.1267E-03	-8.5327E-03	4.3354E-03	i = 1
3	-5.3166E-01	4.5043E-02	2.3246E-04	-2.9578E-03	-3.9322E-04	
4	9.4538E-03	-1.3877E-02	5.2268E-03	3.4957E-03	-1.9477E-03	
1	2.3833E-01	1.6411E-01	3.5264E-02	1.1035E-02	1.9679E-03	
2	-9.7385E-05	-6.8034E-05	9.6643E-06	-5.6311E-06	-5.4057E-06	i = 2
3	7.4594E-02	4.0510E-02	7.1444E-03	1.8741E-03	1.9290E-04	
4	1.5814E-04	2.4653E-05	-2.0128E-05	2.1969E-06	1.6462E-06	
1	-8.4895E-02	-6.0406E-02	-1.3958E-02	-4.4421E-03	-4.3691E-04	
2	3.8333E-05	2.7750E-05	-1.9421E-06	2.4539E-06	2.0217E-06	i = 3
3	-3.7465E-02	-2.0201E-02	-3.0003E-03	1.3477E-04	2.3811E-04	
4	-6.5564E-05	-1.1191E-05	4.0144E-06	-5.4225E-07	-5.8000E-07	

k (row label for the left side)

(a) j = 1

Table XIX (continued)

k		l = 1	2	3	4	5	
	1	-4.8751E 00	3.8568E-01	8.9416E-02	-3.8336E-03	-5.6381E-04	
	2	-5.9249E-02	3.5900E-02	-1.0355E-02	-1.0107E-02	5.2158E-03	$i = 1$
	3	-2.5328E-01	4.9919E-02	-1.1629E-03	-6.2057E-04	1.9001E-04	
	4	1.0344E-02	-1.6060E-02	6.3760E-03	4.0934E-03	-2.3237E-03	
	1	2.9309E-02	2.2488E-02	3.3054E-03	-7.9395E-04	-3.0994E-04	
	2	-1.6327E-04	-1.0971E-04	1.5669E-05	-8.7017E-06	-6.7401E-06	$i = 2$
	3	1.1645E-02	-8.6387E-04	-1.2205E-03	-4.9475E-04	-1.0509E-04	
	4	2.1841E-04	1.0117E-05	-2.8250E-05	4.7106E-06	1.9140E-06	
	1	-1.0665E-02	-7.2509E-03	6.4902E-04	1.6192E-03	5.3594E-04	
	2	6.2224E-05	4.2486E-05	-4.6543E-06	2.6943E-06	2.2411E-06	$i = 3$
	3	-3.2906E-03	2.7208E-03	1.8934E-03	4.2051E-04	1.1062E-05	
	4	-8.6335E-05	-2.1279E-06	1.1893E-05	-1.5278E-06	-7.5504E-07	

(b) $j = 2$

Table XIX (concluded)

k		ℓ				
		1	2	3	4	5
	1	-3.4190E-02	3.0987E-03	2.1003E-04	-1.3227E-04	3.8909E-05	
	2	-1.6852E-02	1.1232E-02	-3.4617E-03	-2.9578E-03	1.5737E-03	i = 1
	3	2.7661E-02	4.6634E-03	-2.3584E-03	4.1068E-05	8.9787E-05	
	4	2.5474E-03	-4.4827E-03	1.9705E-03	1.1712E-03	-6.8976E-04	
	1	6.4502E-03	3.0166E-03	-7.0828E-04	-4.5555E-04	-8.0377E-05	
	2	-7.8057E-05	-5.0343E-05	7.3723E-06	-3.6923E-06	-2.1734E-06	i = 2
	3	7.4611E-04	-4.4199E-04	-1.6938E-04	2.8031E-05	7.0774E-06	
	4	8.2677E-05	-8.5206E-06	-1.0920E-05	2.6752E-06	5.4410E-07	
	1	-1.5477E-03	5.6917E-04	1.4176E-03	3.8754E-04	8.4904E-06	
	2	2.8730E-05	1.8310E-05	-3.0414E-06	5.9468E-07	5.5401E-07	i = 3
	3	4.5921E-04	1.0043E-03	2.8368E-04	-1.2268E-04	-5.5630E-05	
	4	-3.0280E-05	6.1870E-06	4.8664E-06	-1.1045E-06	-2.6257E-07	

(c) j = 3

84

Table XX
Deflection Lead Coefficients

	1	2	3	4	
1	-3.9351E-02	-1.2398E-02	8.9290E-03	4.6850E-03	
2	-3.0070E-01	1.8807E 00	-2.4089E-02	-1.1390E-01	i = 1
3	-1.9928E-02	7.4787E-05	6.7211E-03	-1.5203E-04	
4	6.5680E-03	-3.9599E-02	-1.3457E-02	7.4622E-03	
1	2.2500E-04	-7.1265E-05	-4.7970E-04	1.6094E-04	
2	1.5998E-01	-3.2743E-03	7.2055E-02	-1.8383E-02	i = 2
3	-1.6292E-07	5.1229E-05	-2.0231E-04	1.3498E-05	
4	2.6840E-02	-7.3312E-03	5.1992E-03	-3.9343E-05	
1	-9.5671E-05	3.5257E-05	2.2675E-04	-8.4850E-05	
2	-5.3962E-02	3.6225E-03	-4.0943E-02	1.0932E-02	i = 3
3	7.9258E-07	-2.3174E-05	7.9057E-05	-2.0696E-06	
4	-1.6931E-02	5.2690E-03	3.9336E-03	-2.7604E-03	

k (row label, left side)

ℓ (column header, top)

(a) j = 1

Table XX (continued)

l

	1	2	3	4	
1	-4.6841E-02	-1.0797E-02	1.0742E-02	4.4299E-03	
2	2.4711E-02	1.1543E 00	-3.0148E-02	-8.1854E-02	
3	-2.3469E-02	2.8899E-03	8.1240E-03	-1.1396E-03	$i = 1$
4	1.6340E-02	-2.9855E-02	-5.5323E-03	5.8674E-03	
1	2.7947E-04	-9.6353E-05	-5.8091E-04	1.6886E-04	
2	1.0158E-02	8.4111E-03	-9.3709E-04	-5.7418E-03	
3	1.6586E-06	1.9142E-06	-2.5927E-04	4.7605E-05	$i = 2$
4	1.0662E-03	-2.4102E-03	1.4989E-03	-1.6803E-03	
1	-1.1936E-04	4.6571E-05	2.8064E-04	-1.0206E-04	
2	-3.3991E-03	-5.1704E-03	-1.0901E-03	6.8922E-03	
3	-2.4804E-07	8.1187E-07	1.0221E-04	-2.6085E-05	$i = 3$
4	-4.7029E-04	1.6250E-03	-4.0849E-04	9.7372E-04	

k (row label)

(b) $j = 2$

Table XX (concluded)

	ℓ 1	2	3	4	
1	-1.3805E-02	-8.3727E-04	3.7319E-03	6.2461F-04	
2	7.9195E-02	1.7003E-02	-2.1836E-02	-4.6020E-03	$i = 1$
3	-7.1968E-03	2.5078E-03	2.4563E-03	-9.0335F-04	
4	3.6638E-03	-3.9977E-03	-1.2238E-03	1.7201E-03	
1	9.0090E-05	-3.4113F-05	-1.7808E-04	3.6458E-05	
2	4.2095E-03	6.3808E-04	-2.4189E-03	-2.8192E-04	$i = 2$
3	6.1834E-07	-3.4613E-05	-8.6951E-05	3.2838F-05	
4	1.7608E-04	-3.9705E-04	2.7399E-04	1.6422E-05	
1	-3.8453E-05	1.6571E-05	4.6956F-05	-3.0613F-05	
2	-1.8315E-03	3.4524F-05	1.9185E-03	1.1758E-04	$i = 3$
3	-3.5444E-07	1.7119F-05	3.4371E-05	-2.1768F-05	
4	6.4209E-05	3.1245E-04	-2.5297E-04	-5.1228E-05	

k

(c) $j = 3$

REFERENCES

1. Norwood, John M., The Approximate Equations For Large Yaw Trajectory Tables. Report No. MPRL 515. Military Physics Research Laboratory, The University of Texas, Austin, Texas, 31 May 1960, (Unclassified).

2. Norwood, John M., A Review of the Method of Siacci Trajectory Computation for Airborne Gunfire. ARL-TM-71-27. Applied Research Laboratories, The University of Texas at Austin, Austin, Texas, August 1971, (Unclassified).

3. Morgan, Ellis F., A Modified Siacci Method Applied to High-Yaw, 20-MM, M56 Shell Ballistic Computations for Airborne Gunnery. Report No. ARL-TR-71-47. Applied Research Laboratories, The University of Texas at Austin, Austin, Texas, October 1971, (Unclassified).

4. Norwood, John M., and Ellis F. Morgan, Modified Point-Mass Equations for Calculating Large-Yaw Trajectories in Airborne Gunnery Systems. Report No. ARL-TR-71-52. Applied Research Laboratories, The University of Texas at Austin, Austin, Texas, October 1971, (Unclassified).

5. Sterne, Theodore, The Effect of Yaw Upon Aircraft Gunfire Trajectories. Report No. BRL R 345. Ballistic Research Laboratories, Aberdeen Proving Ground, Maryland, June 1943, (Unclassified).

6. Nielsen, Kaj L., and James F. Heyda, The Mathematical Theory of Airborne Fire Control. NAVORD Report 1493. Bureau of Ordnance, U. S. Navy, Washington, D.C., 20 July 1951, (Unclassified).

7. Morgan, Ellis, F., and John M. Norwood, Direct N-Dimensional Polynomial Curve Fitting of Ballistic Lead Angles for a Flexible Gun. Report No. ARL-TM-71-24. Applied Research Laboratories, The University of Texas at Austin, Austin, Texas, June 1971, (Unclassified).

8. McShane, Edward J., John L. Kelly, and Franklin V. Reno, Exterior Ballistics. The University of Denver Press, 1953.

9. Norwood, John M., and Ellis F. Morgan, Tables of Siacci Functions for the 20-mm, M56 Shell. Report No. ARL-TM-71-25. Applied Research Laboratories, The University of Texas at Austin, Austin, Texas, August 1971, (Unclassified).

10. Ballistic Data Based on the Drag Function for the 20-mm Shell, HEI, T282E1. Report No. 018. Air Proving Ground Command, Eglin Air Force Base, Florida, (Unclassified).

11. Lebegern, Charles H., Jr., Ballistic Data for Cartridge HEI, 20-mm, M56 Fired with Large Yaw from High Altitude Aircraft. BRL Report No. 1136. Ballistic Research Laboratories, Aberdeen Proving Ground, Maryland, April 1958, (Unclassified).

12. Garrett, G. S., et al., Seventh Quarterly Technical Note (November, December, 1961, and January 1962). MPRL Report No. 547. Military Physics Research Laboratory, The University of Texas, Austin, Texas, February 1962, (Unclassified).

13. Ratcliff, R. R., M. O. Glasgow, Ballistic Data for the 20-mm, M55,HEI Projectiles Fired with Large Yaw Angles from the M61 Gun. Armament Memorandum Report 69-13. Air Force Armament Laboratory, Air Force Systems Command, Eglin Air Force Base, Florida, September 1969, (Unclassified).

Distribution List for AFAL-TR-73-179

ADDRESSEE	COPIES
Activities at WPAFB, OH 45433	
AFAL/XP	1
AFAL/NV	1
AFAL/NVT-1	10
AFAL/NVA-598DF	1
AFAL/TSR	1
ASD/YF	1
ASD/YB	1
ASD/SD-4	1
ASD/ENVW	1
2750 ABW/SSL	1
Other	
Hq USAF/SAMID Washington, D. C. 20330	1
Hq USAF/SAGF 1111 19th Street Arlington, VA 22209	1
AFATL/DLD Eglin AFB, FL 32542	1
AFATL/DLY Eglin AFB, FL 32542	1
Hq TAC/DR Langley AFB, VA 23365	1
USAFTFWC Nellis AFB, NV 89110	1

ADDRESSEE	COPIES
Hq ADC/XP Ent AFB, CO 80912	1
ADWC/4750 TES-P Tyndall AFB, FL 32401	1
USAFA/DFASTRO Colorado Springs, CO 80840	1
Air University Library Maxwell AFB, AL 36112	1
Commander Naval Weapons Center China Lake, CA 94555	1
Point Mugu Naval Air Station Attn: Lt Cdr Teague Point Mugu, CA 93041	1
Commander Naval Weapon Lab/MAL Dahlgren, VA 22448	1
Director, Development Center Marine Corps Development & Education Center Air Operations Division Quantico, VA 22134	1
Ballistic Research Laboratories Attn: Mr. C. H. Lebegern Aberdeen Proving Ground, MD 21005	1
Frankford Arsenal Attn: Mr. G. H. Sigman Philadelphia, PA 19101	1
Defense Documentation Center Cameron Station Alexandria, VA 22314	2
Applied Research Laboratories The University of Texas at Austin Attn: Mr. John W. Carlson Austin, TX 78712	2

ADDRESSEE	COPIES
Applied Research Laboratories The University of Texas at Austin Attn: Technical Library Austin, TX 78712	1

DOCUMENT CONTROL DATA - R & D		
Security classification of title, body of abstract and indexing annotation must be entered when the overall report is classified)		
1. ORIGINATING ACTIVITY *(Corporate author)* Aerospace Technology Division Applied Research Laboratories The University of Texas at Austin, Austin, Texas	2a. REPORT SECURITY CLASSIFICATION Unclassified	
	2b. GROUP	

3. REPORT TITLE

COMPARISON OF APPROXIMATE METHODS FOR AIRBORNE GUNNERY
BALLISTICS CALCULATIONS

4. DESCRIPTIVE NOTES *(Type of report and inclusive dates)*
Technical Report

5. AUTHOR(S) *(First name, middle initial, last name)*

John M. Norwood

6. REPORT DATE April 1973	7a. TOTAL NO. OF PAGES xiv + 89	7b. NO. OF REFS 13
8a. CONTRACT OR GRANT NO. F33615-70-C-1162 b. PROJECT NO.	9a. ORIGINATOR'S REPORT NUMBER(S) ARL-TR-73-10	
c. d.	9b. OTHER REPORT NO(S) *(Any other numbers that may be assigned this report)* AFAL-TR-73-179	

10. DISTRIBUTION STATEMENT

Distribution limited to U.S. Government agencies only; (Test and Evaluation);
(statement applies April 1973). Other requests for this document must be
referred to AFAL-NVT-1.

11. SUPPLEMENTARY NOTES	12. SPONSORING MILITARY ACTIVITY Air Force Avionics Laboratory Wright-Patterson Air Force Base Ohio 45433

13. ABSTRACT

   A new, simplified set of approximate, large-yaw, ballistic trajectory equations
are derived for airborne gunnery applications in which corrections for yaw drag and
windage jump are included. The results of computations done with the new set of
equations are in excellent agreement with the results of calculations done with the
approximate equations used at Eglin Air Force Base to generate trajectory tables.
Comparisons are made for the 20-mm, M56 round. A reduction in computer time
by a factor of 15 to 20 (depending on firing geometry) over the Eglin set of equations
can be expected when the simplified set of equations is used. The new set of equa-
tions is almost as simple as particle trajectory equations and is a candidate set for
onboard calculations.

   When the yaw-drag and windage-jump corrections are used with the Siacci
method, a closed-form solution to the ballistic trajectory equations is obtained. This
method is almost as accurate as the simplified set of equations above, except for
time-of-flight calculations. If time of flight is not important, as, for example, in
air-to-ground applications, then this method yields results of sufficient accuracy out
to moderate ranges for most geometries. Also, this method appears to be 20 to
100 times as fast as point-mass integration and 500 to 1500 times as fast as numer-
ical integration of the Eglin approximate equations of motion.

   A method of polynomial curve fitting of ballistic lead angles for air-to-ground
applications is presented. This method may be useful in situations where onboard
calculations are not possible.

DD FORM 1473 (PAGE 1)

S/N 0101-807-6801

KEY WORDS	LINK A		LINK B		LINK C	
	ROLE	WT	ROLE	WT	ROLE	WT
Exterior Ballistics						
Trajectories						
Firing Tables						
Fire Control						